

Critical examination of RHIC paradigms—mostly high p_T

Michael J. Tannenbaum^{*†}

Physics Dept., 510c, Brookhaven National Laboratory, Upton, NY 11973-5000, USA

E-mail: mjt@bnl.gov

A critical examination of RHIC paradigms is presented. Topics include: search for a critical point with a low energy scan; the lack of understanding of radiative processes in a medium in QCD compared in detail to examples from QED; the reason why some physicists started to measure particles at large p_T in the 1960's; a review of the discovery of hard-scattering in p-p collisions in the 1970's via single-inclusive and two-particle correlations and application of these techniques at RHIC. Several paradigms in both soft and hard physics which are popular at RHIC are discussed and challenged.

Workshop on Critical Examination of RHIC Paradigms

April 14-17, 2010

Austin, Texas, U.S.A.

^{*}Speaker.

[†]Supported by the U.S. Department of Energy, Contract No. DE-AC02-98CH1-886.

1. The Quark Gluon Plasma (QGP)

Let me start out with the famous schematic plots of the phase diagram of nuclear matter Fig. 1 [1, 2]. The presumed trajectories of the evolution of the medium for collisions at RHIC and LHC c.m.

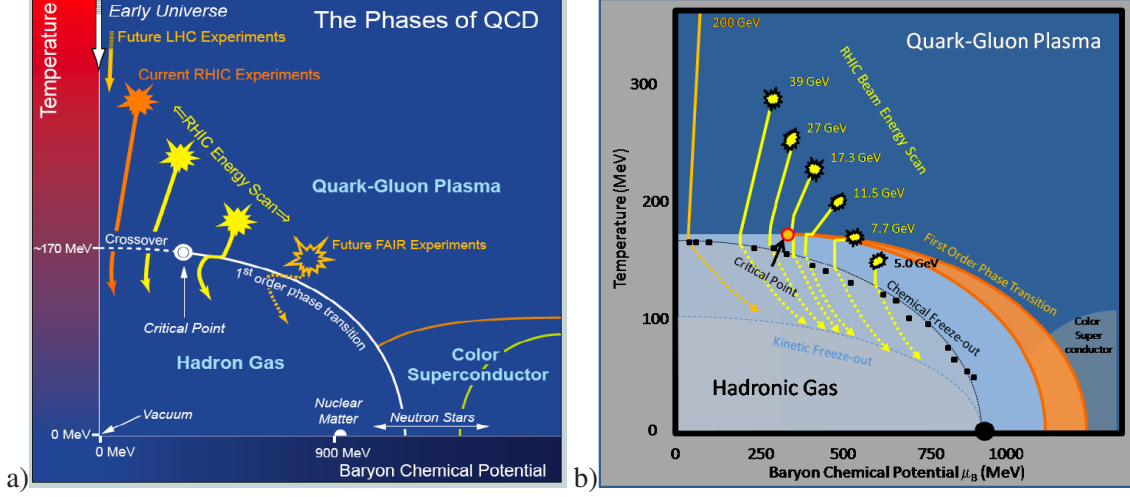


Figure 1: a) A schematic representation of the QCD Phase Diagram [1]. b) The location of the critical point, the separation between the 1st-order transition and chemical freeze-out, and the focusing of the event trajectories towards the critical point, are not based on specific quantitative predictions, but are all chosen to illustrate plausible possibilities [2]

energies are shown in Fig. 1a, where the axes are the temperature T vs. the baryon chemical potential μ_B . The temperature for the transition from the Quark Gluon Plasma (QGP) to a hadron gas is taken as 170 MeV for $\mu_B = 0$ and the phase boundary is predicted to be a smooth crossover down to a critical point below which the phase boundary becomes a first order phase transition. Also shown are idealized trajectories for the RHIC c.m. energy scan and future experiments at FAIR which are being performed in order to find the QCD critical point.

One paradigm that I don't believe is that one can find the critical point by an energy scan at RHIC. Luciano Moretto at WWND2010 said, "critical fluctuations depend on a first order phase transition below the critical point whose large fluctuations drive the critical fluctuations", leading me to ask again whether all the interesting physics just outside the E802 aperture? What I mean by this is that since no fluctuations, other than from known correlations such as Bose-Einstein interference, were observed at the AGS fixed target Au+Au program at c.m. energy $\sqrt{s_{NN}} = 4.8$ GeV (see below), or from the CERN Pb+Pb fixed target program at c.m. energy $\sqrt{s_{NN}} = 17.2$ GeV (Fig. 2a) [3, 4] there is no first order phase transition to drive the critical fluctuations. Specifically, from AGS to RHIC energies, the non-random fluctuations of M_{pT} , the event-by-event average p_T , are about 1% of the $\langle p_T \rangle$, averaged over all events, independent of $\sqrt{s_{NN}}$ (Fig. 2b) [5, 6] and show no evidence of fluctuations from a first-order phase transition. The only escape is if the QGP can not be reached in A+A collisions below the critical point, i.e. the endpoints of the trajectories in Fig. 1b for $\sqrt{s_{NN}} = 17.2$ GeV and below lie between the Chemical Freeze-out line and the phase-boundary. In principle, this is possible, but in my opinion it is very unlikely given the constancy of

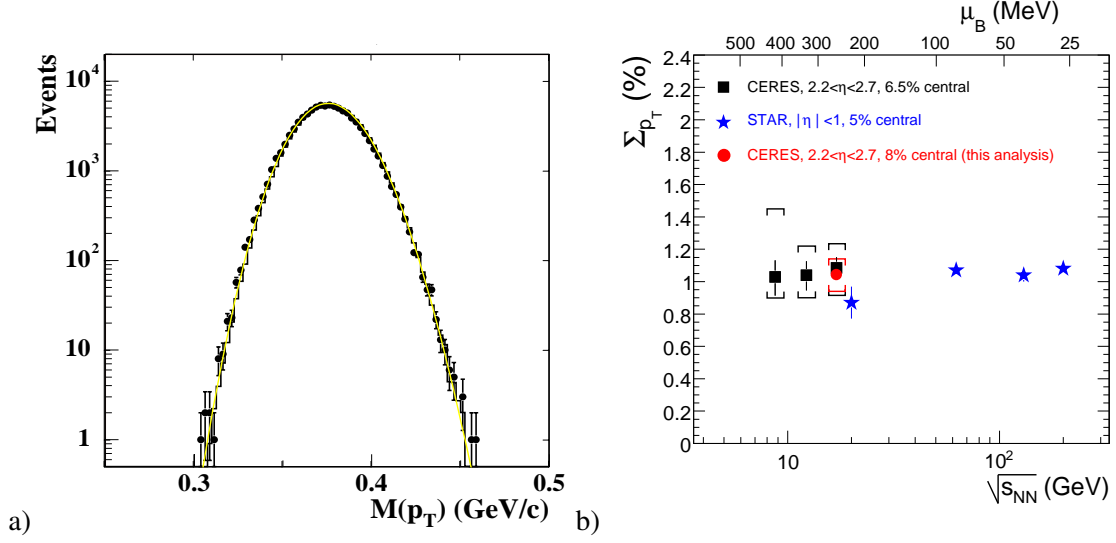


Figure 2: a) Distribution of event-by-event average p_T , $M_{p_T} = \overline{p_T} = \frac{1}{n} \sum_{i=1}^n p_{T_i}$, where n is the number of particles on a given event, in 158 GeV/nucleon Pb+Pb collisions (data points); histogram is from mixed events [3]. Line is calculated random convolution of inclusive p_T spectrum [4]. b) rms/mean of M_{p_T} distribution with random effect subtracted, $\Sigma_{p_T} = \sqrt{\frac{\sigma_{M_{p_T}}^2}{\langle p_T \rangle^2} - \left(\frac{\sigma_{M_{p_T}}^2}{\langle p_T \rangle^2} \right)_{\text{random}}}$ as a function of $\sqrt{s_{NN}}$ [6].

Σ_{p_T} as a function of $\sqrt{s_{NN}}$ in Fig. 2b.

2. Given the Quark Gluon Plasma (QGP), what is my interest?

The QGP is the only place in the universe where we can in principle and in practice understand QCD for color-charged quarks in a color-charged medium. How long will it take before we understand a quark in a QCD medium as well as we understand the passage of a muon through Copper in QED (Fig. 3)?

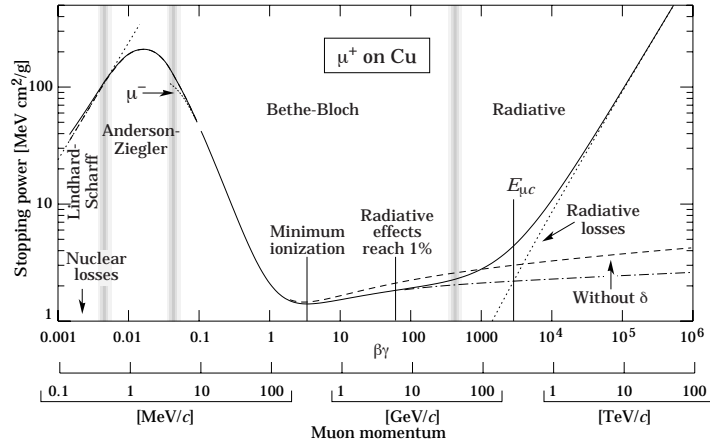


Figure 3: dE/dx of a μ^+ in Copper as a function of muon momentum [7].

2.1 QED Bremsstrahlung in matter and crystals

Even for such a seemingly simple reaction as muon bremsstrahlung, there is no simple formula [8]. For bremsstrahlung of an electron of energy E in a solid, apart from the standard Bethe-Heitler radiation ($kdN/dk = d/X_o$, where k =energy of radiated photon and d/X_o =the thickness in radiation lengths, X_o), there are also very interesting effects [9]: the Landau-Pomeranchuk-Migdal (LPM) effect, which decreases the radiation at low $x = k/E$; transition radiation at low x ; and a medium effect on the forward outgoing photon from Compton scattering off the atomic electrons which if inside the coherence length kills the dN/dk divergence. The coherence length is set by t_{\min} . For bremsstrahlung of a photon with energy k by a particle with mass m , energy E :

$$\frac{1}{L_{coh}} = q_L = \sqrt{t_{\min}} = \frac{m^2 k}{2E(E-k)} \quad (2.1)$$

where $q = \sqrt{|t|}$ is the 4-momentum transfer to the target. Figure 4a [9] shows the bremsstrahlung spectrum of equivalent photons, kdN/dk , from 8 GeV electrons incident on a 3% radiation length (X_o) Aluminum target. The pure Bethe-Heitler spectrum, $kdN/dk = d/X_o$ is shown by the dashed line. Inclusion of the LPM suppression gives the dotted line. Further inclusion of the dielectric

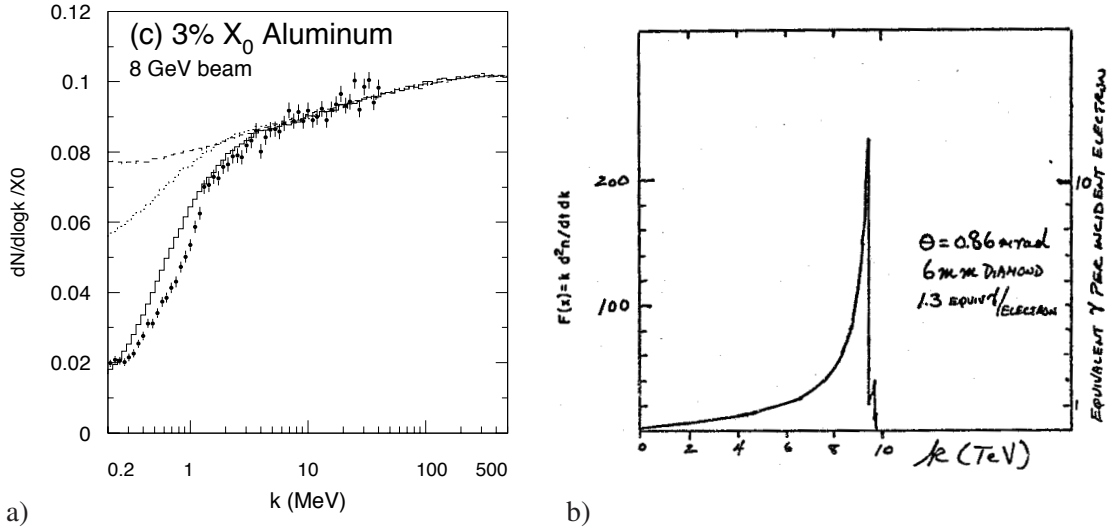


Figure 4: a) SLAC measurement of equivalent photon spectrum kdN/dk in 3% X_o Al target [9] illustrating LPM and dielectric suppression at low $x = k/E$. b) Calculation of coherent bremsstrahlung in a diamond crystal with a peak at 9.48 TeV for a proposed 10 TeV electron beam at the SSC [11].

suppression gives the histogram, which agrees with the measurement. For crystals, there is also coherent bremsstrahlung when the momentum transfer vector \vec{q} equals a characteristic momentum of the reciprocal lattice (Bragg condition) which greatly increases the radiation [10] as shown in Fig. 4b [11].

I hope that the discussion in this section has illustrated the point that the understanding of dE/dx for quarks and gluons in a QGP, which is much more complicated than for leptons and photons in solids in QED, is in its infancy and has barely scratched the surface.

3. Why were some people studying “high p_T ” physics in the 1960’s

The quick answer is that they were looking for a ‘left handed’ intermediate boson W^\pm , the proposed carrier of the weak interaction [12].

The first opportunity to study weak interactions at high energy was provided by the development of neutrino beams at the new accelerators in the early 1960’s, the CERN-SPS and the BNL-AGS [13] where the μ -neutrino was discovered [14]. However, it was soon recognized that the intermediate (weak) boson, W^\pm might be more favorably produced in p-p collisions [15]. The canonical method for discovering the W -boson in p-p collisions was described by Nino Zichichi in a comment at the 1964 ICHEP, which deserves a verbatim quote because it was exactly how the W was discovered at CERN 19 years later [18, 19]: “We would observe the μ ’s from W -decays. By measuring the angular and momentum distribution at large angles of K and π ’s, we can predict the corresponding μ -spectrum. We then see if the μ ’s found at large angles agree with or exceed the expected numbers.” I became aware of this “Zichichi signature” in my graduate student days when I checked the proceedings of the 12th ICHEP in Dubna, Russia in 1964 to see how my thesis results were reported [16] and I found several interesting questions and comments by an “A. Zichichi” printed in the proceedings (Fig. 5). The W is still being measured by this method at RHIC (Fig. 6) [22] except now we use polarized p-p collisions and can measure the parity violation

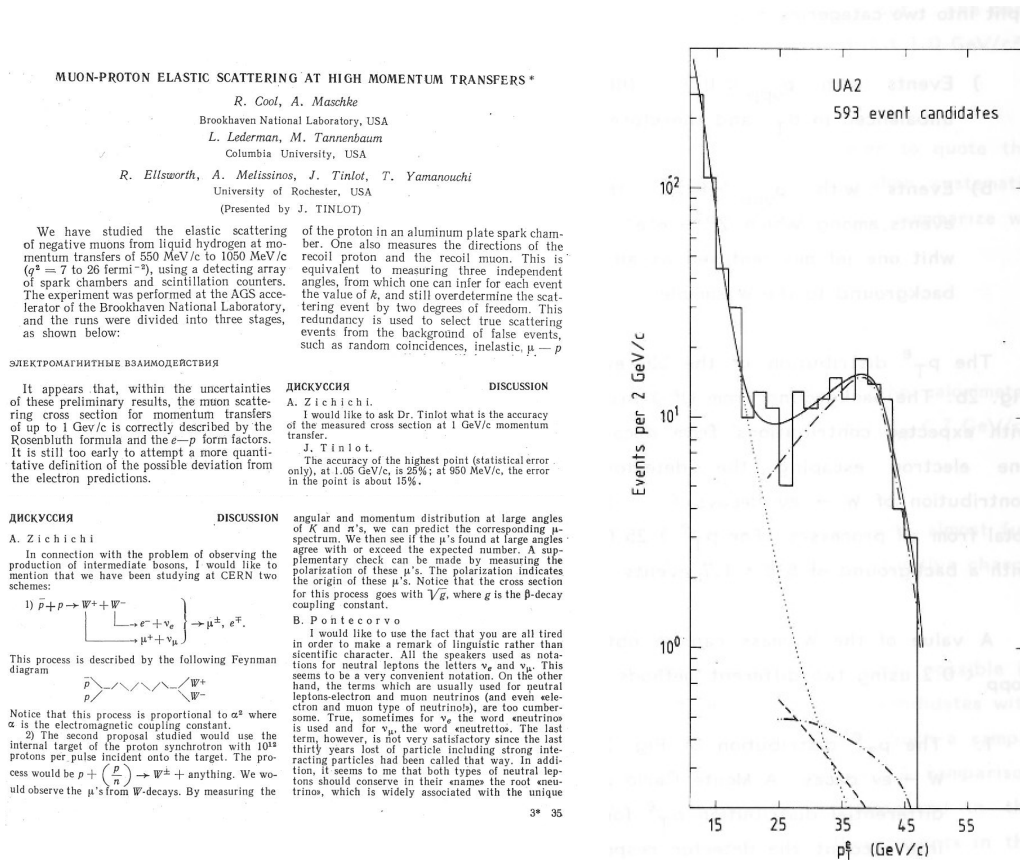


Figure 5: a)(left)Zichichi ICHEP 1964 [16, 17] and b)(right) $W \rightarrow e + \nu$ from UA2 [20] 1982-1984 runs, about 1/4 of the final sample [21]

in W production which will enable us to measure flavor identified spin structure functions of \bar{u} and \bar{d} quarks [23]. Now back to the mid 1960's

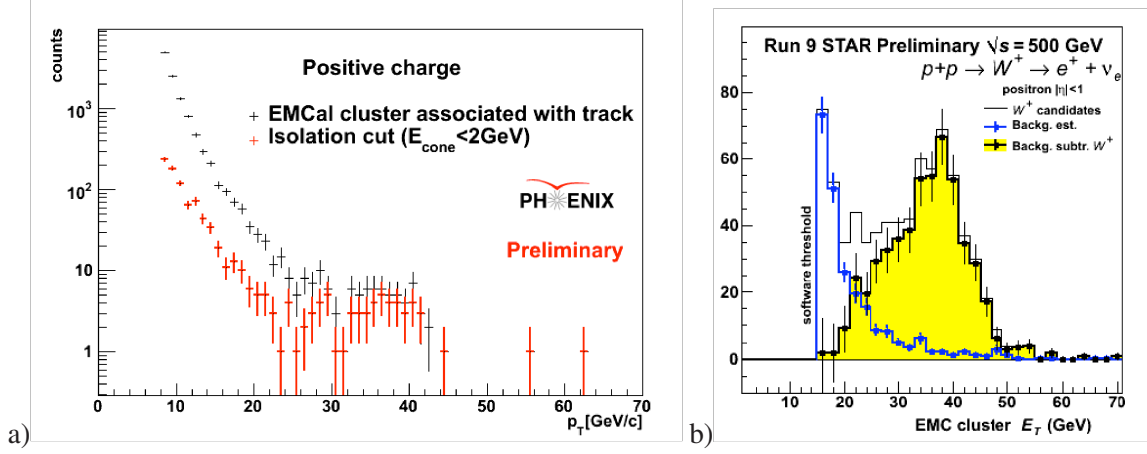


Figure 6: PHENIX (a) and STAR (b) preliminary results [22] for $W^+ \rightarrow e^+ + X$ from a short run at RHIC of polarized p-p collisions at $\sqrt{s} = 500 \text{ GeV}$ in 2009. The parity violation in real W^+ production has been measured for the first time with this data to $\sim 4.0\sigma$ significance, combined.

3.1 The absence of high p_T single leptons leads to lepton-pair measurements.

Proton-beam-dump experiments at the ANL-ZGS [24] and BNL-AGS [25, 26] looking for “large angle” muons didn’t find any. Then the big question became, “How do you know how many W ’s should have been produced?”. Chilton Saperstein and Shrauner [27] emphasized the need to know the timelike form factor of the proton in order to calculate the W production rate; and Yamaguchi [28] proposed that the timelike form factor could be found by measuring the number of lepton pairs (e^+e^- or $\mu^+\mu^-$), “massive virtual photons”, of the same invariant mass as the W (but also noted that the individual leptons from these electromagnetically produced pairs might mask the leptons from the W). This set off a spate of single and di-lepton experiments, notably the discovery by Lederman *et al.* of “Drell-Yan” pair production at the BNL-AGS [29, 30] followed by the experiments E70 and CCR at the new FNAL-Tevatron and CERN-ISR machines, respectively.

The discovery of “Drell-Yan” pairs at the AGS proved to be seminal in future Relativistic Heavy Ion Physics as well as providing an interesting lesson. Figure 7a) shows the di-muon invariant mass spectrum $d\sigma/dm_{\mu\mu}$ from the collisions of 29.5 GeV protons in a thick Uranium target. There was definitely a dispute in the group about the meaning of the shoulder or “bump” or “??” for $2.5 < m_{\mu\mu} < 4.0 \text{ GeV}/c^2$, which was apparently resolved adequately by the long forgotten theory paper [31] which produced the curve that beautifully agreed with the data (Fig. 7b) with the explanation, “The origin of the shoulder comes from an interplay between the phase-space control of the integration region and the q^2 dependence of the coefficient.” The important lesson that I learned from Fig. 7 is to NEVER be influenced by theoretical curves which “explain” your data. It is only when the curves fail to explain the data that you learn something definitive: the theory is wrong.

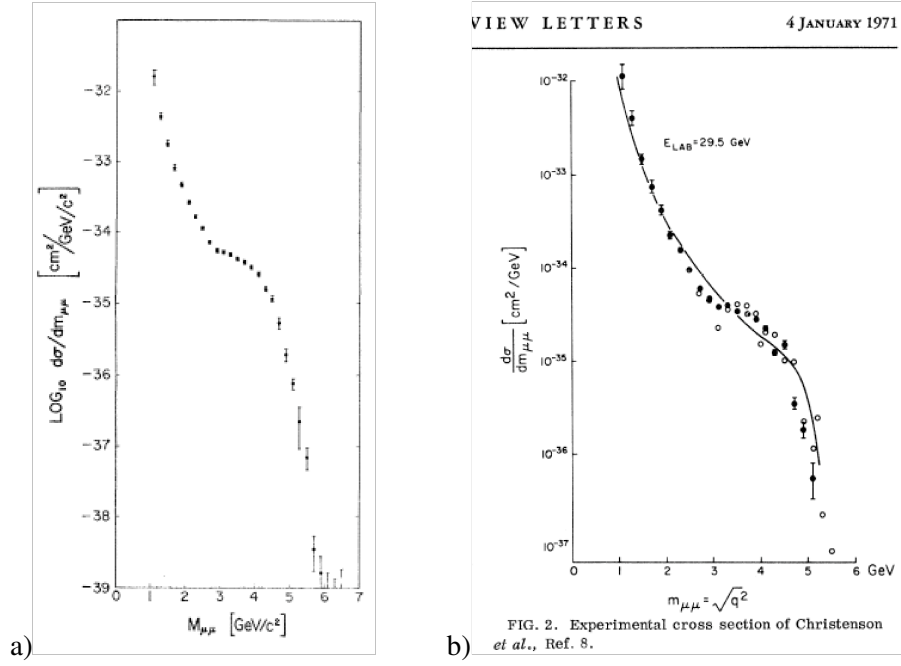


Figure 7: a) Dimuon invariant mass spectrum $d\sigma/dm_{\mu\mu}$ [29]; b) theoretical prediction [31] for $d\sigma/dm_{\mu\mu}$.

Leon Lederman was very excited in 1970 to be in the possession of the di-muon continuum mass spectrum, $d\sigma/dm_{\mu\mu}$, because by combining this result at $\sqrt{s} = 7.4$ GeV with the newly found Bjorken Scaling [32] as used by Drell and Yan [30], he could calculate the W cross section at any \sqrt{s} , and hence the sensitivities of his two proposals E70 [33] and CCR [34] (see Fig. 8). Details worthy of note from Fig. 8b are the e^{-6p_T} pion yield, the line with the worst imaginable background and the Jacobean peaks at $p_T = M_W/2$ from $W \rightarrow e + X$ for various W masses.

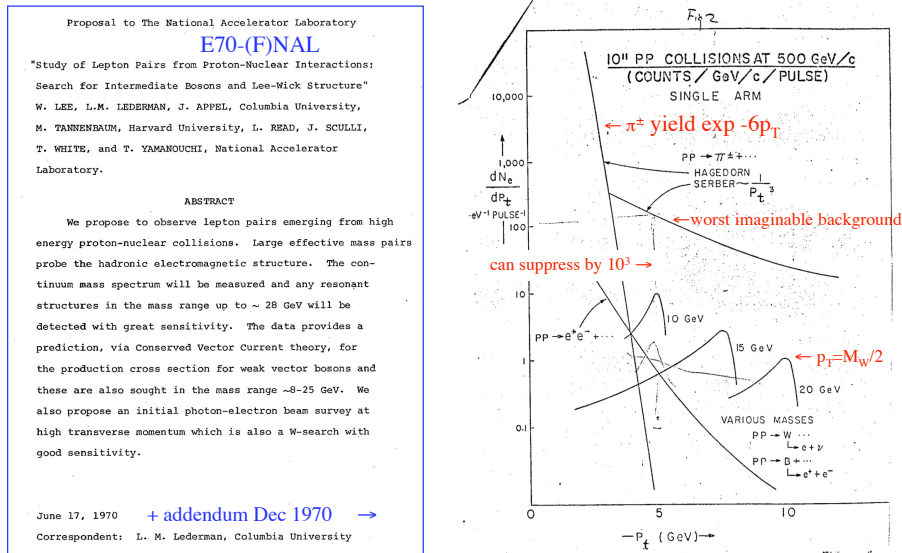
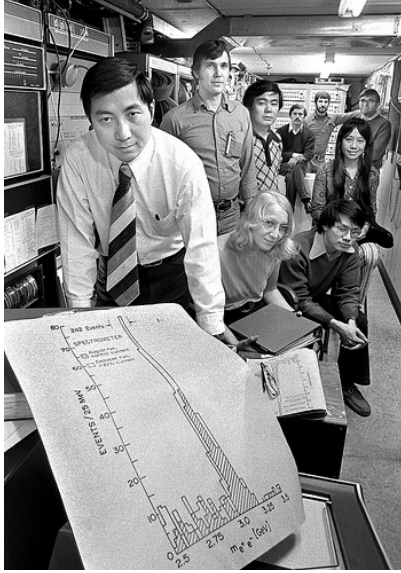


Figure 8: a) (left) Proposal for E70 Fermilab, June 17, 1970; b) (right) Cross section and background calculation for $W^\pm \rightarrow e^\pm + X$ from Addendum [33].

4. The November Revolution and Birth of a QGP Paradigm

Lederman’s shoulder was explained in November 1974 by the discovery of the J/ψ at the BNL-AGS [35] and at SLAC [36] (Fig. 9). This discovery revolutionized high energy physics since it was a heavy vector meson with a very narrow width (it decayed slowly) which implied a new



VOLUME 33, NUMBER 23

PHYSICAL REVIEW LETTERS

2 DECEMBER 1974

Experimental Observation of a Heavy Particle J/ψ

J. J. Aubert, U. Becker, P. J. Biggs, J. Burger, M. Chen, G. Everhart, P. Goldhagen, J. Leung, T. McCulliston, T. G. Rhoades, M. Rohde, Samuel C. C. Ting, and Sau Lan Wu
Laboratory for Nuclear Science and Department of Physics, Massachusetts Institute of Technology,
Cambridge, Massachusetts 02139

and

Y. Y. Lee
Brookhaven National Laboratory, Upton, New York 11973
(Received 12 November 1974)

We report the observation of a heavy particle J/ψ , with mass $m = 3.1$ GeV and width approximately zero. The observation was made from the reaction $p + \text{Be} \rightarrow e^+ + e^- + x$ by measuring the e^+e^- mass spectrum with a precise pair spectrometer at the Brookhaven National Laboratory's 30-GeV alternating-gradient synchrotron.

This experiment is part of a large program to study the behavior of timelike photons in $p + p \rightarrow e^+ + e^- + x$ reactions and to search for new particles which decay into e^+e^- and $\mu^+\mu^-$ pairs.

daily with a thin Al foil. The beam spot size is 3×6 mm², and is monitored with closed-circuit television. Figure 1(a) shows the simplified side view of one arm of the spectrometer. The two

Discovery of a Narrow Resonance in e^+e^- Annihilation*

J.-E. Augustin,† A. M. Boyarski, M. Breidenbach, F. Bulos, J. T. Dakin, G. J. Feldman, G. E. Fischer, D. Fryberger, G. Hanson, B. Jean-Marie,† R. R. Larsen, V. Lith, H. L. Lynch, D. Lyon, C. C. Morehouse, J. M. Paterson, M. L. Perl, B. Richter, P. Rapidis, R. F. Schwitters, W. M. Tanenbaum, and F. Vannucci

Stanford Linear Accelerator Center, Stanford University, Stanford, California 94305

and

G. S. Abrams, D. Briggs, W. Chinowsky, C. E. Friedberg, G. Goldhaber, R. J. Hollebeek, J. A. Kadyk, B. Lulu, F. Pierre,§ G. H. Trilling, J. S. Whitaker, J. Wiss, and J. E. Zipse

Lawrence Berkeley Laboratory and Department of Physics, University of California, Berkeley, California 94720
(Received 13 November 1974)

We have observed a very sharp peak in the cross section for $e^+e^- \rightarrow \text{hadrons}$, $e^+\mu^-$, and possibly $\mu^+\mu^-$ at a center-of-mass energy of 3.105 ± 0.003 GeV. The upper limit to the full width at half-maximum is 1.3 MeV.

Figure 9: (left) Sam Ting with J discovery at BNL; (right) J [35] and ψ [36] discoveries in PRL

conservation law, similar to the discovery of strange particles in cosmic rays [37]. The J/ψ was quickly understood to be a bound state of heavy $c - \bar{c}$ quarks (charmonium) [38]—the hydrogen atom of QCD. This was clear evidence for a “2nd” generation of quarks, and made all physicists believe in quarks and QCD. This discovery also changed the paradigm of di-lepton production from the measurement of background for W production to the search for new resonances. Greatly improved di-muon measurements by E70 in 1977 in p+A collisions at Fermilab [39] set the standard for di-muon production (Fig. 10a) and were rewarded with the discovery of an even heavier “3rd” generation of quark, the b -quark [39]. At CERN, di-muon measurements were extended to h+A collisions by NA3 [40] and NA10 [41] and then to Pb+Pb collisions by NA50 (Fig. 10b) [42, 43].

4.1 J/ψ suppression as the first paradigm for detecting the QGP

In 1986, Matsui and Satz [44] proposed that due to the Debye screening of the color potential in a QGP, charmonium production would be suppressed since the $c - \bar{c}$ quarks couldn’t bind. This paradigm drove the field of RHI physics for two decades; and the observation of J/ψ suppression in A+A collisions [45, 43] is the CERN fixed target Heavy Ion program’s claim to fame. However, the interpretation is not straightforward because the J/ψ is suppressed in p+A collisions (see Fig. 11). The PHENIX experiment at RHIC was specifically designed to measure J/ψ production at rest at mid-rapidity in p-p and Au+Au collisions [46] and found the same J/ψ suppression at $\sqrt{s_{NN}} = 200$ GeV as found at $\sqrt{s_{NN}} = 17.2$ GeV (158A GeV bombarding energy) at CERN by

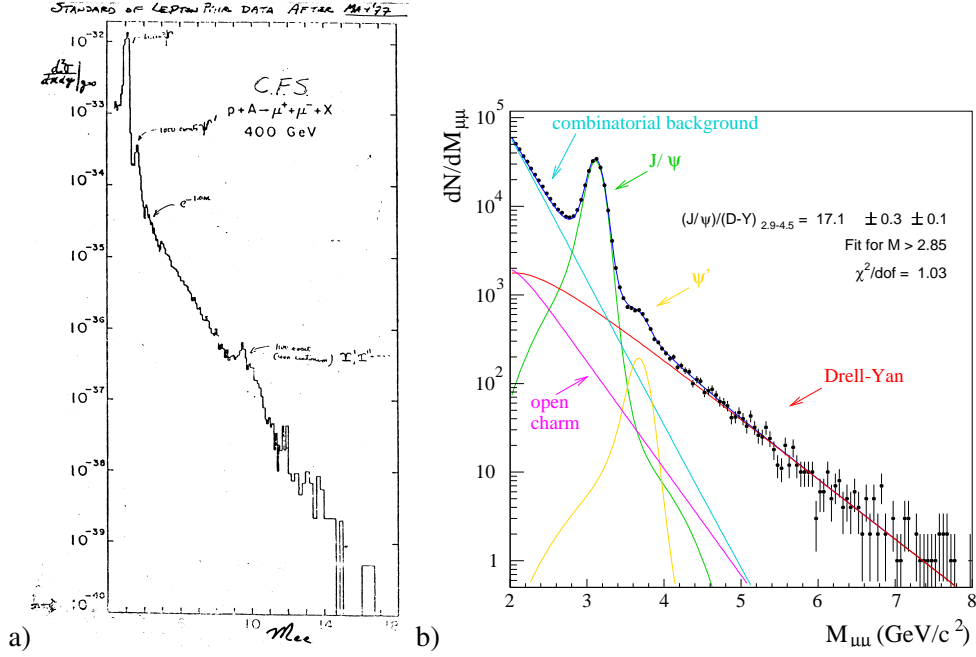


Figure 10: a) CFS di-muon spectrum at $\sqrt{s_{NN}}=27.4$ GeV [39], with J/ψ , ψ' , Υ clearly seen along with the Drell-Yan continuum, $d\sigma/dm \propto e^{-1.0m}$. b) NA50 di-muon spectrum in 158A GeV Pb+Pb collisions [42]

NA50 [43], further complicating the J/ψ -suppression ‘paradigm’. Incredibly, the CERN fixed target RHI program is still making progress, having (after 21 years [45]) finally measured the p+A cold nuclear matter effect for J/ψ at the same incident energy, 158 GeV, as for Pb+Pb [47] (compare Fig. 11), which materially changes the result. At best, the J/ψ -suppression paradigm is presently inconclusive. Hopefully, results from the LHC may settle the issue [48].

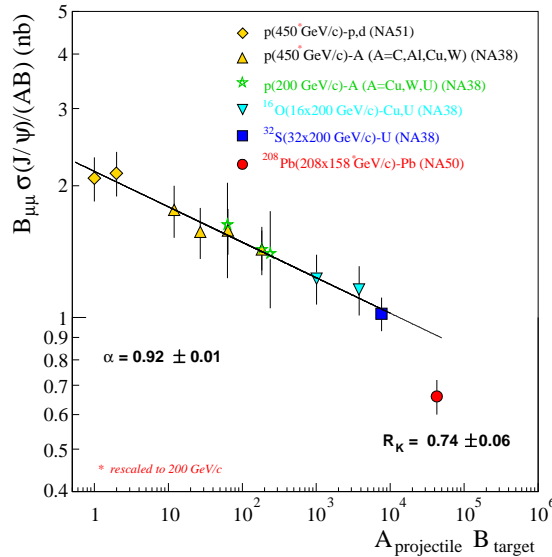


Figure 11: The $J/\psi \rightarrow \mu^+\mu^-$ cross section in A+B collisions divided by $A \times B$ [42]. Line is $(AB)^\alpha$ with $\alpha = 0.92 \pm 0.01$. Only the Pb+Pb data fall below this line. However, note the *.

5. A second paradigm for detecting the QGP, BDMPSZ [49, 50] 1997–1998

In 1998, at the QCD workshop in Paris, Rolf Baier asked me whether jets could be measured in Au+Au collisions because he had a prediction of a QCD medium-effect (energy loss via gluon radiation induced by multiple scattering [51]) on color-charged partons traversing a hot-dense-medium composed of screened color-charges [52]. I told him [53] that there was a general consensus [54] that for Au+Au central collisions at $\sqrt{s_{NN}} = 200$ GeV, leading particles are the only way to find jets, because in one unit of the nominal jet-finding cone, $R = \sqrt{(\Delta\eta)^2 + (\Delta\phi)^2}$, there is an estimated $\pi R^2 \times \frac{1}{2\pi} \frac{dE_T}{d\eta} \sim 375$ GeV of energy (!)

The good news was that hard-scattering in p-p collisions had been discovered at the CERN ISR [55–57] by the method of leading particles, before the advent of QCD, and it was proved by single inclusive and two-particle correlation measurements in the period 1972–1978 that high p_T particles are produced from states with two roughly back-to-back jets which are the result of scattering of constituents of the nucleons as described by QCD, which was developed during this period. The other good news was that these techniques could be used to study hard-scattering and jets in Au+Au collisions and that the PHENIX detector had been designed to make such measurements and could trigger, measure and separate γ and π^0 out to $p_T > 25$ GeV in p-p and Au+Au collisions. In fact, in many talks, dating from as long ago as 1979 [58], I have been on record describing “How everything you want to know about jets can be found using 2-particle correlations”.¹

One lesson from this new paradigm is that a good probe of QCD in a fundamental system such as p-p collisions (Fig. 12) provides a well calibrated probe of QCD in more complicated collisions such as Au+Au. In the 1980’s when RHIC was proposed, hard processes were not expected to play a major role in A+A collisions. However, starting in 1997 [61], inspired by Rolf and collaborators, and before them by the work of Gyulassy [62] and Wang [63], I indicated that my best bet on discovering the QGP was to utilize semi-inclusive π^0 or π^\pm production in search for “high p_T suppression”.

5.1 Soft vs. hard-physics in p-p collisions

Fig. 12a nicely illustrates two important points for π^0 production in p-p collisions. Apart from the beautiful data, the main emphasis is the agreement of NLO pQCD with the measurement for $p_T \gtrsim 3$ GeV/c. Actually this surprised some of my colleagues from the lepton-scattering community, but was no surprise to me because such data in the 1970’s is what made people believe in QCD (see Sec. 7 below). The other important issue is the transition from the exponential “soft physics” spectrum for $p_T < 1.5$ GeV/c to the power law spectrum of hard scattering at larger p_T . The $e^{-5.5p_T}$ exponential at $\sqrt{s} = 200$ GeV, is very close to the original cosmic-ray “Cocconi Formula” [66], e^{-6p_T} , used by Lederman (Fig. 8b) in 1970, but the power-law hard-scattering spectrum for $p_T > 3$ GeV/c is much larger than the “worst imaginable background”. This is the hard-scattering component which I shall discuss again below but I first wish to emphasize some important issues in Relativistic Heavy Ion physics which are dominated by the soft physics.

¹Recently, I had to amend this statement to ‘almost everything’ because we found that the fragmentation function can not be measured in di-hadron correlations because the two particles, e.g. $\pi^0 - h$, are both fragments of jets [59, 60] (see Secs. 7.3, 8.2.1 below).

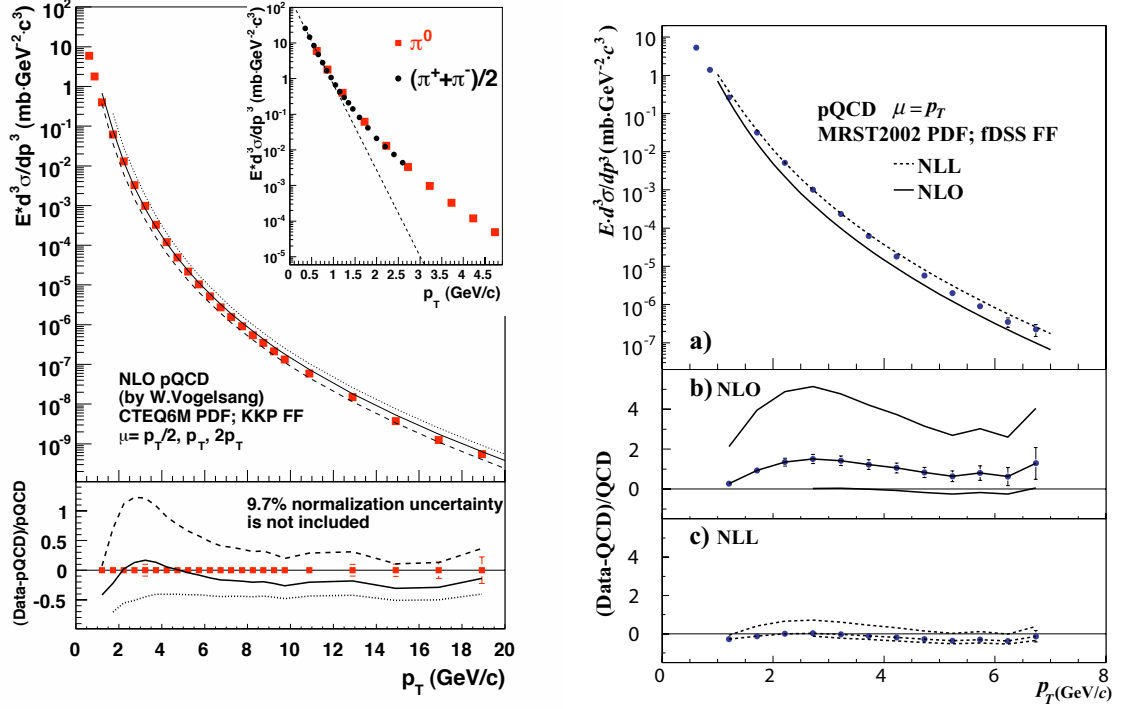


Figure 12: (left) PHENIX measurement of invariant cross section, $Ed^3\sigma/d^3p$, as a function of transverse momentum p_T for π^0 production at mid-rapidity in p-p collisions at c.m. energy $\sqrt{s} = 200$ GeV [64]. (right) PHENIX measurement of π^0 in p-p collisions at $\sqrt{s} = 62.4$ GeV [65].

6. The important of soft-physics in Relativistic Heavy Ion Collisions

In dealing with Relativistic Heavy Ions, there are three dramatic differences from p-p physics.

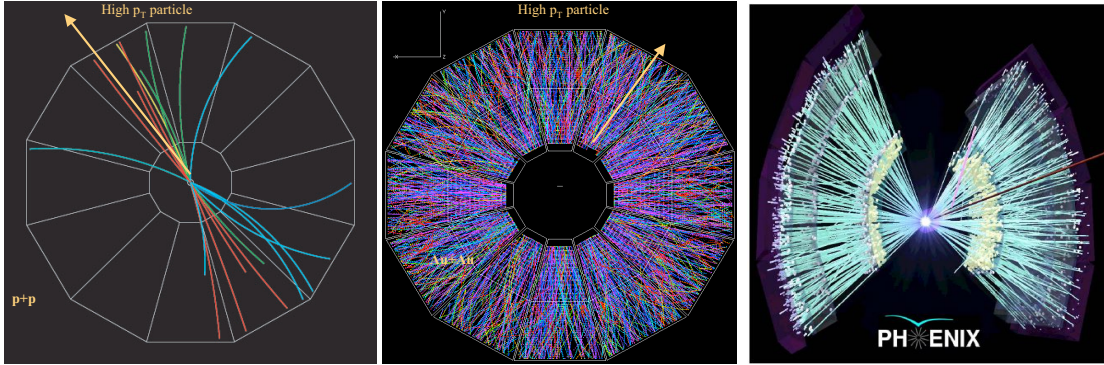


Figure 13: a) (left) A p-p collision in the STAR detector viewed along the collision axis; b) (center) Au+Au central collision at $\sqrt{s_{NN}} = 200$ GeV in the STAR detector; c) (right) Au+Au central collision at $\sqrt{s_{NN}} = 200$ GeV in the PHENIX detector.

- The particle multiplicity is $\sim A$ times larger in A+A central collisions than in p-p collisions (Fig. 13). This is why there is such a huge energy, $\sim 375 R^2$ GeV, in a jet cone of radius R at $\sqrt{s_{NN}} = 200$ GeV.

- There are huge azimuthal anisotropies in A+A which don't exist in p-p which are interesting in themselves, and are useful, but sometimes can be troublesome.
- Space-time issues, both in momentum space and coordinate space are important in RHI. For example:
 1. When in time and space does a parton fragment? Is this different for light and heavy quarks? When are particles formed?
 2. The Dokshitzer textbook formula, $\tau_F = ER^2$, should, I think, be corrected to $\tau_F = \gamma R = R \times E/M = ER\lambda_C$, where R , M , are the radius and mass of the particle and λ_C its Compton wavelength.
 3. Would a proton embedded in a QGP dissolve? How long does this take? How is this related to J/ψ suppression?

6.1 Soft physics dominates multi-particle production in both p-p and A+A collisions

A quantity related to multiplicity, but more relevant for the study of jets, is the distribution of transverse energy, $E_T = \sum_i E_i \sin \theta_i$, where the sum is taken over all particles emitted on an event into a fixed but large solid angle, typically measured in a calorimeter, corrected for the calorimeter response and then corrected to the solid angle $\Delta\eta = 1$, $\Delta\phi = 2\pi$ [67]. E_T is also related to M_{pT} , the event-by-event average p_T (Fig. 2a), except that it is the sum of p_T of all particles on every event rather than the average. dE_T/dy is thought to be related to the co-moving energy density in a longitudinal expansion [69, 68], and taken by all experiments as a measure of the energy density in space, “the Bjorken energy density”, ε_{Bj} :

$$\varepsilon_{Bj} = \frac{d\langle E_T \rangle}{dy} \frac{1}{\tau_F \pi R^2} \quad (6.1)$$

where τ_F , the formation time, is usually taken as 1 fm/c, $\pi R^2 = A_\perp$ is the transverse overlap area of the collision, and $d\langle E_T \rangle/dy$ is the co-moving energy density.

The main importance of E_T distributions in RHI collisions (see Fig. 14a) is that they are sensitive primarily to the nuclear geometry of the reaction, and hence can be used to measure the centrality of individual interactions on an event-by-event basis.² Thus, the transverse energy or multiplicity distribution in A+A collisions has a characteristic shape which is quite different from that in p-p collisions since it is sensitive to the number of participants or centrality of an A+A collision and integrates over all impact parameters. This is shown in Fig. 14a for Au+Au collisions at AGS ($\sqrt{s_{NN}} = 5.4$ GeV) and RHIC ($\sqrt{s_{NN}} = 200$ GeV), together with an estimate at RHIC for p-p collisions. The fact that the scaled AGS and RHIC E_T distributions lie one on top of each other shows that the shape of E_T distributions is essentially entirely dominated by the nuclear-geometry at both the AGS and RHIC; which implies that there are no critical fluctuations at either the AGS or RHIC. Above the upper 0.5 percentile of the distribution ($E_T \approx 710$ GeV on Fig. 14), measurements in smaller solid angles show increasingly larger fluctuations represented by flatter slopes above the knee of the distribution; but this is a random fluctuation (fewer particles in

²However, in PHENIX, centrality is determined far from mid-rapidity to avoid possibly biasing any of the mid-rapidity measurements.

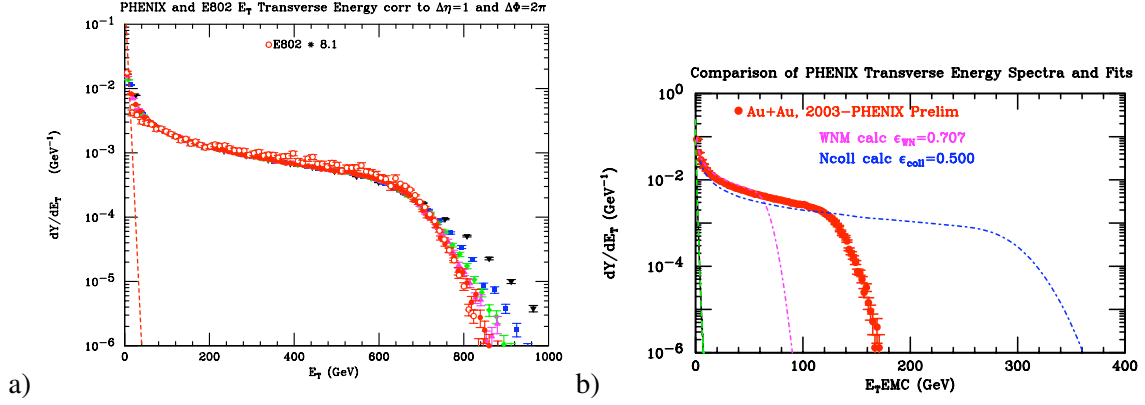


Figure 14: a) E_T distributions in Au+Au collisions: PHENIX at $\sqrt{s_{NN}} = 200$ GeV [70] compared to the E802 (non-response-corrected) E_T at $\sqrt{s_{NN}} = 5.4$ GeV [71, 72] scaled up by 8.1. The quantity plotted is the normalized yield, dY/dE_T (GeV^{-1}), which integrates to 1, i.e. $\int dE_T dY/dE_T = 1$. Different filled symbols represent PHENIX measurements in solid angles $\Delta\eta = 0.76$, $\Delta\phi = m \times \pi/8$ at mid rapidity with $m = 1, \dots, 5$. Dashed line is an estimate of E_T distribution in p-p collisions at $\sqrt{s} = 200$ GeV for $m = 5$. b) PHENIX $m = 5$ raw E_T distribution, $E_{T,EMC}$, at $\sqrt{s_{NN}} = 200$ GeV together with calculated distributions for participant scaling, WNM ($E_T \propto N_{\text{part}}/2$), and Ncoll scaling ($E_T \propto N_{\text{coll}}$) based on convolutions of the p-p distribution.

the smaller solid angle fluctuate more). This is visible only for the most central collisions when the nuclear-geometrical fluctuations have saturated (all nucleons participating). The Bjorken energy density can be straightforwardly computed from Fig. 14a at RHIC ($\sqrt{s_{NN}} = 200$ GeV), with $\epsilon_{Bj} \times \tau_F = 5.4 \pm 0.6$ GeV/fm^2 [70] for the 5% most central collisions ($E_T \geq 580$ GeV). For the AGS data, the ratio of 8.1 shown in Fig. 14 can not be used to get $\epsilon_{Bj} \times \tau_F$ at $\sqrt{s_{NN}} = 5.4$ GeV because the E802 data have not been corrected for the calorimeter response, which is much more difficult in the fixed target geometry. However, Ref. [70] calculated the fully corrected E802 E_T from charged particle measurements and obtained $\epsilon_{Bj} \times \tau_F = 1.0$ GeV/fm^2 at $\sqrt{s_{NN}} = 4.8$ GeV.

6.2 Another paradigm we should do away with

It has been popular to characterize the average values of $dE_T/d\eta$ (or the charged multiplicity density $dn^{ch}/d\eta$) in A+A collisions as a function of centrality by the equation [73, 74]

$$dn_{AA}^{ch}/d\eta = (1-x) dn_{pp}^{ch}/d\eta \times N_{\text{part}}/2 + x dn_{pp}^{ch}/d\eta \times N_{\text{coll}} \quad . \quad (6.2)$$

While this may seem reasonable for the average value $\langle dn_{AA}^{ch}/d\eta \rangle$ at a given centrality, is nonsense for the distribution, which if such a representation were true would be the weighted sum of $(1-x) \times$ the WNM curve + $x \times$ the Ncoll curve in Fig. 14b, which obviously looks nothing like the actual $E_{T,EMC}$ measurement. (A more reasonable representation is $dn_{AA}^{ch}/d\eta \propto N_{\text{part}}^\alpha$.) Also the claim that the Ncoll scaling of the *soft* p-p E_T or multiplicity n_{pp}^{ch} distributions (or average values) in Eq. 6.2 has anything to do with hard-scattering [74] is equally nonsensical. This could be further elaborated by looking for jets in the p-p data; but such measurements (not finding jet activity until 4-5 orders of magnitude down in E_T cross section) were already done by COR [75] and UA2 [76] 25 years ago (see Fig. 21 below).

6.3 Another soft-physics paradigm to test at the LHC—Hydrodynamics

In my opinion, the most interesting soft physics issue for the LHC concerns the possible increase of the anisotropic flow v_2 beyond the ‘hydrodynamic limit’. Wit Busza’s extrapolation [77] of v_2 to the LHC energy is shown in Fig. 15a, a factor of 1.6 increase from RHIC. A previous

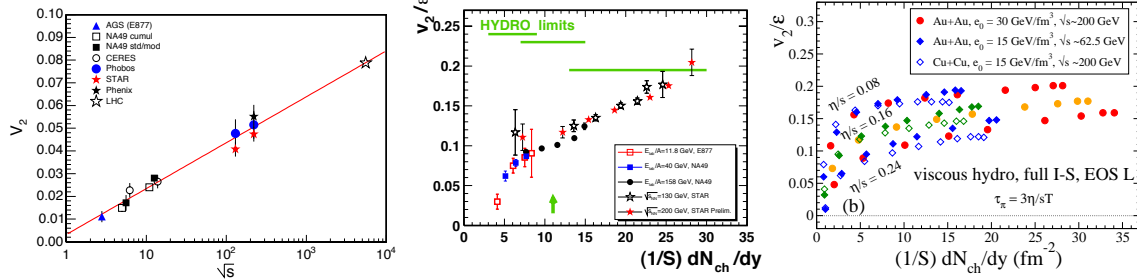


Figure 15: a) (left) Busza’s extrapolation of v_2 to LHC [77]. b) (center) v_2/ϵ vs ‘Bjorken multiplicity density’, $(1/S)dN_{ch}/dy$ [78]. c) (right) ‘Hydro Limit’ calculated in viscous Hydrodynamics for several values of the initial energy density e_0 [79].

paper by NA49 [78] which compared v_2 measurements from AGS and CERN fixed target experiments to RHIC as a function of the ‘Bjorken multiplicity density’, $dn_{ch}/d\eta/S$, where S is the overlap area of the collision zone, showed an increase in v_2/ϵ from fixed target energies to RHIC leading to a “hydro limit”, where ϵ is the eccentricity of the collision zone (Fig. 15b). This limit was confirmed in a recent calculation by Uli Heinz using viscous relativistic hydrodynamics [79] which showed a clear hydro-limit of $v_2/\epsilon = 0.20$ (Fig. 15c). This limit is sensitive to the ratio of the viscosity/entropy density, the now famous η/s , but negligibly sensitive to the maximum energy density of the collision, so I assume that this calculation would give a hydro-limit at the LHC not too different from RHIC, $v_2/\epsilon \approx 0.20$. Busza’s extrapolation of a factor of 1.6 increase in v_2 from RHIC to LHC combined with v_2/ϵ from Fig. 15b gives $v_2/\epsilon = 0.32$ at LHC. In my opinion this is a measurement which can be done to high precision on the first day of Pb+Pb collisions at the LHC, since it is high rate and needs no p-p comparison data. Personally, I wonder what the hydro aficionados would say if both Heinz’ and Busza’s predictions were correct?

7. Hard-Scattering in p-p collisions

We now go back to where we were in the search for high p_T leptons and di-leptons before we got diverted by the J/ψ discovery (and QGP paradigm) and soft-physics issues.

7.1 Bjorken scaling and the parton model

The idea of hard-scattering in p-p collisions dates from the first indication of pointlike structure inside the proton, in 1968, found at SLAC by deeply inelastic electron-proton scattering [80], i.e. scattering with large values of 4-momentum transfer squared, Q^2 , and energy loss, ν . The discovery that the Deeply Inelastic Scattering (DIS) structure function

$$F_2(Q^2, \nu) = F_2\left(\frac{Q^2}{\nu}\right) \quad (7.1)$$

“scaled” i.e just depended on the ratio

$$x = \frac{Q^2}{2Mv} \quad (7.2)$$

independently of Q^2 , as originally suggested by Bjorken [32], led to the concept of a proton composed of point-like ‘partons’ [81]. The deeply inelastic scattering of an electron from a proton is simply quasi-elastic scattering of the electron from point-like partons of effective mass Mx , with quasi-elastic energy loss, $v = Q^2/2Mx$ (Fig. 16a). The probability for a parton to carry a fraction x of the proton’s momentum is measured by $F_2(x)/x$.

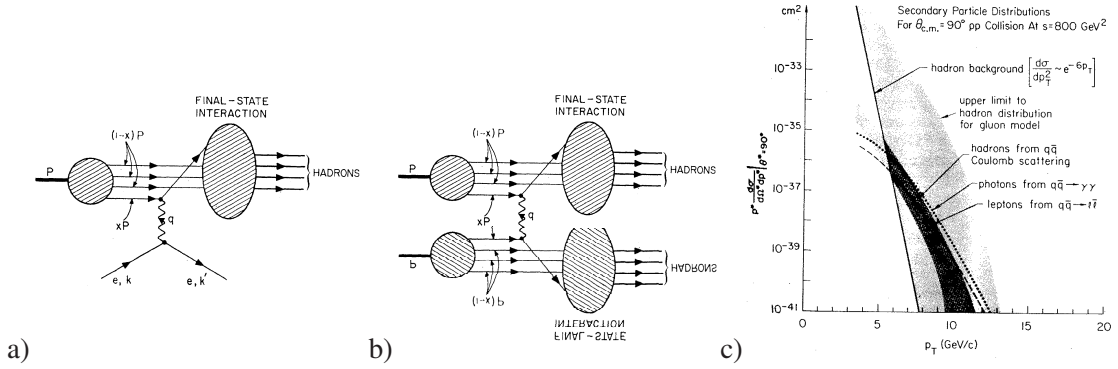


Figure 16: a) Schematic e-p DIS via e-parton scattering [81] b) Schematic parton-parton scattering in p-p c) Predicted cross section according to reaction in (b).

Since the partons of DIS are charged, and hence must scatter electromagnetically from each other in a p-p collision (Fig. 16b), Berman, Bjorken and Kogut (BBK) [82] and subsequent authors [83, 84], derived a general formula for the cross section of the inclusive reaction

$$p + p \rightarrow C + X \quad (7.3)$$

using the principle of factorization of the reaction into parton distribution functions for the protons, fragmentation functions to particle C for the jet of particles from the scattered parton and a short-distance parton-parton hard scattering cross section. The invariant cross section for the inclusive reaction (Eq. 7.3), where particle C has transverse momentum p_T near mid-rapidity was given by the general ‘scaling’ form: [83]

$$E \frac{d^3\sigma}{dp^3} = \frac{1}{p_T^{n_{\text{eff}}}} F\left(\frac{2p_T}{\sqrt{s}}\right) = \frac{1}{\sqrt{s}^{n_{\text{eff}}}} G(x_T) \quad \text{where} \quad x_T = 2p_T/\sqrt{s} \quad (7.4)$$

The cross section has 2 factors, a function F (G) which ‘scales’, i.e. depends only on the ratio of momenta; and a dimensioned factor, $p_T^{-n_{\text{eff}}} (\sqrt{s}^{-n_{\text{eff}}})$, where n_{eff} gives the form of the force-law between constituents. For QED or Vector Gluon exchange [82], $n_{\text{eff}} = 4$, and for the case of quark-meson scattering by the exchange of a quark [83], $n_{\text{eff}}=8$. Using this formalism, BBK predicted (Fig. 16c) hard-scattering must exist in p-p collisions since the charged partons of DIS must scatter electromagnetically, this “electromagnetic contributions may be viewed as a lower bound on the real cross section at large p_T ”.

7.2 Discovery of high p_T π^0 production in p-p collisions

The CERN Columbia Rockefeller (CCR) Collaboration [55] (and also the Saclay Strasbourg [56] and British Scandinavian [57] collaborations) at the CERN-ISR measured pion production over a large range of transverse momenta, unavailable in cosmic ray studies or at lower \sqrt{s} . The e^{-6p_T} soft-spectrum at low p_T which depends very little on \sqrt{s} breaks to a power law at high p_T with a strong and characteristic \sqrt{s} dependence (Fig. 17a). The large rate at high p_T , much larger than expected in Figs. 8b and 16c, indicates that *partons interact strongly ($\gg EM$) with each other*. However, the QED or Vector Gluon form of BBK [82], $p_T^{-4}F(p_T/\sqrt{s})$, was not observed in the experiment but scaling with $n_{\text{eff}} \simeq 8$ was observed (Fig. 17b), which spawned a whole host of new theories. [83]. The first application of QCD to wide angle hadron collisions [84], showed that pure x_T scaling breaks down: n_{eff} varies according to the x_T and \sqrt{s} regions used in the comparison, $n_{\text{eff}} \rightarrow n_{\text{eff}}(x_T, \sqrt{s})$; but this was not enough to resolve $n_{\text{eff}} \simeq 8$ issue, which turned out to be due to “ p_T broadening” by initial state parton transverse momentum, the “ k_T effect.” [85].

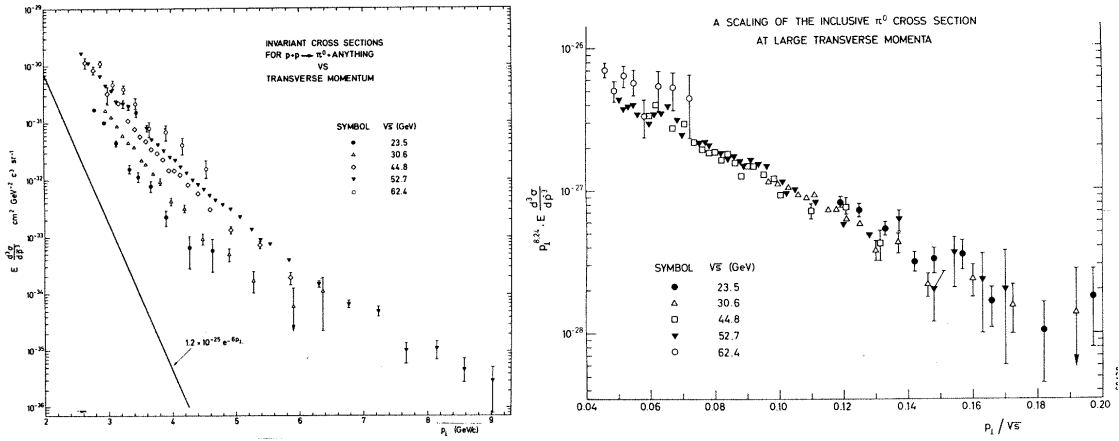


Figure 17: a) (left) CCR [55] transverse momentum dependence of the invariant cross section at five center of mass energies. b) (right) The same data multiplied by p_T^n , using the best fit value of $n = 8.24 \pm 0.05$, with $F = Ae^{-bx_{\perp}}$, plotted vs p_{\perp}/\sqrt{s} .

7.3 Everything you want to know about jets can be found using 2-particle correlations.

Following the discovery of hard-scattering in p-p collisions at the CERN-ISR by single particle inclusive measurements, the attention of experimenters turned to measuring the predicted di-jet structure of the hard-scattering events using two-particle correlations. At the CERN-ISR, from 1975–1982, two-particle correlations showed unambiguously that high p_T particles come from di-jets. The outgoing jet-pair of hard-scattering obeys the kinematics of elastic-scattering (of partons) in a parton-parton c.m. frame which is longitudinally moving with rapidity $y = (1/2) \ln(x_1/x_2)$ in the p-p c.m. frame. Hence, the jet-pair formed from the scattered partons should be co-planar with the beam axis, with two jets of equal and opposite transverse momentum. Thus, the outgoing jet-pair should be back-to-back in azimuthal projection. It is not necessary to fully reconstruct the jets in order to measure their properties. In many cases two-particle correlations are sufficient to measure the desired properties. Many ISR experiments provided excellent 2-particle correlation

measurements [86]. However, the CCOR experiment [87] was the first to provide charged particle measurement with full and uniform acceptance over the entire azimuth, with pseudorapidity coverage $-0.7 \leq \eta \leq 0.7$, so that the jet structure of high p_T scattering could be easily seen and measured.

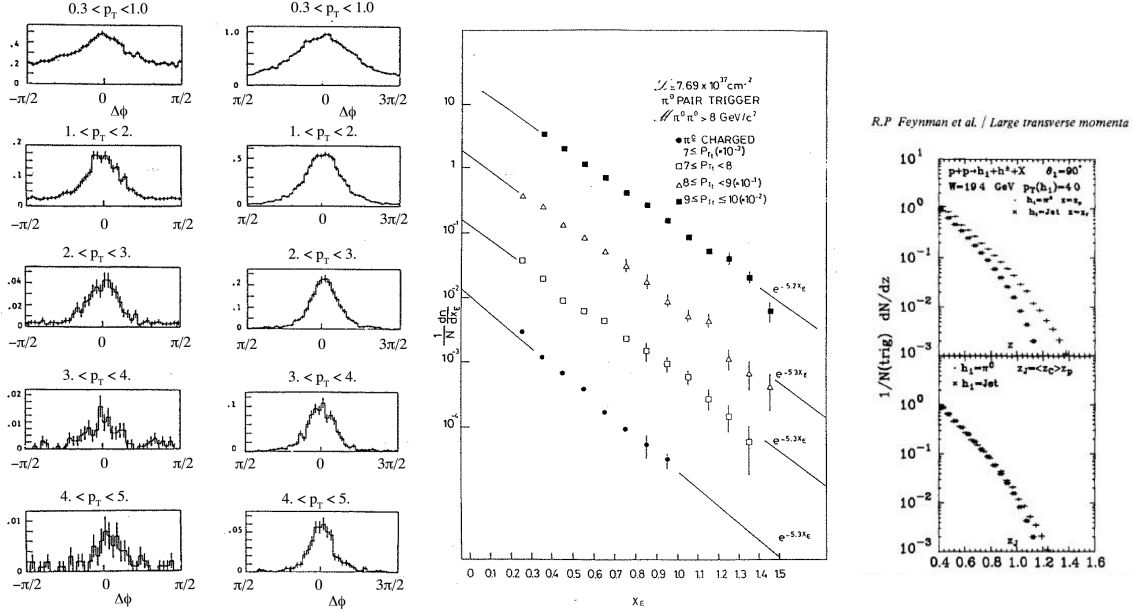
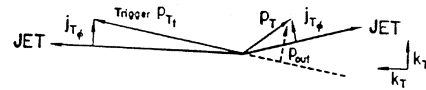


Figure 18: a) (left) trigger-side ($\Delta\phi = \pm\pi/2$) b) (left-center) away-side ($\Delta\phi = \pm\pi/2$ around π rad.) correlations of charged particles with indicated $p_T \equiv p_{T_a}$ for π^0 triggers with $p_{T_t} \geq 7$ GeV/c, for 5 intervals of p_T ; c) (right-center) x_E distributions from this data. d) right) [top] Comparison [90] of away side charged hadron distribution triggered by a π^0 or a jet, where $z_{\pi^0} = x_E$ and $z_j = p_{T_a}/\hat{p}_{T_a}$. [bottom] same distributions with π^0 plotted vs $z'_j = \langle z_t \rangle x_E$.

The azimuthal distributions of associated charged particles relative to a π^0 trigger with transverse momentum $p_{T_t} > 7$ GeV/c are shown (Fig. 18a,b) for five intervals of associated particle transverse momentum p_T . In all cases, strong correlation peaks on flat backgrounds are clearly visible, indicating the di-jet structure which is contained in an interval $\Delta\phi = \pm 60^\circ$ about a direction towards and opposite to the trigger for all values of associated p_T (> 0.3 GeV/c) shown. The small variation of the widths of the away-side peaks for $p_T > 1$ GeV/c (Fig. 18b) indicates out-of-plane activity of the di-jet system beyond simple jet fragmentation (the k_T effect [85]).

Following the methods of previous CERN-ISR experiments [88, 89] and the best theoretical guidance [90], the away jet azimuthal angular distributions of Fig. 18b, which were thought to be unbiased, were analyzed in terms of the two variables: $p_{\text{out}} = p_T \sin(\Delta\phi)$, the out-of-plane transverse momentum of a track, and x_E :

$$x_E = \frac{-\vec{p}_T \cdot \vec{p}_{T_t}}{|\vec{p}_{T_t}|^2} = \frac{-p_T \cos(\Delta\phi)}{p_{T_t}} \simeq \frac{z}{z_t}$$



where $z_t \simeq p_{T_t}/\hat{p}_{T_t}$ is the fragmentation variable of the trigger jet with \hat{p}_{T_t} , and $z_a \simeq p_{T_a}/\hat{p}_{T_a}$ is the fragmentation variable of the away jet (with \hat{p}_{T_a}). Note that x_E would equal the fragmentation fraction z of the away jet, for $z_t \rightarrow 1$, if the trigger and away jets balanced transverse momentum,

i.e. if $\hat{x}_h \equiv \hat{p}_{T_a}/\hat{p}_{T_t} = 1$. It was generally assumed, following the seminal article of Feynman, Field and Fox [90], that the p_{T_a} distribution of away side hadrons from a single particle trigger [with p_{T_t}], corrected for $\langle z_t \rangle$, would be the same as that from a jet-trigger and follow the same fragmentation function as observed in e^+e^- or DIS [91]. The x_E distributions [87, 92] for the data of Fig. 18b are shown in Fig. 18c and show the fragmentation behavior expected at the time, $e^{-6z} \sim e^{-6x_E \langle z_t \rangle}$. Also, relevant to a recent claim [93], Fig. 18c from 1979 showed that there were no di-jets each of a single particle, as claimed by another ISR experiment [94], since there is no peak at $x_E = 1$.

As noted previously¹, the title of this section should start with “Almost” because we subsequently learned at RHIC [59] that the x_E distribution from di-hadrons (Fig 18c) does not measure the fragmentation function (see Sec. 8.2.1 below).

7.4 Direct searches for Jets 1975-1982: false claims, confusion, skepticism; finally success.

One of the original reasons for measuring jets in p-p collisions was that it was assumed that the jet cross section would measure the parton cross section without reference to the fragmentation functions. However, due to the fact (which was unknown in the 1970’s) that jets in 4π calorimeters at ISR energies or lower are invisible below $\sqrt{\hat{s}} \sim E_T \leq 25$ GeV [100], there were many false claims of jet observation in the period 1977-1982 [101]. The coup-de-grâce to the concept of finding jet structures in large aperture calorimeters was provided by the first measurement of an E_T distribution in the present usage of the terminology (see Sec. 6.1 above) by the NA5 experiment at CERN (Fig. 19a) [102] who found that “The events selected by the full calorimeter trigger show no dominant jet structure. They appear to originate from processes other than two constituent scattering.” This led to mass confusion in the hard-scattering community in the period 1980-1982 and to great

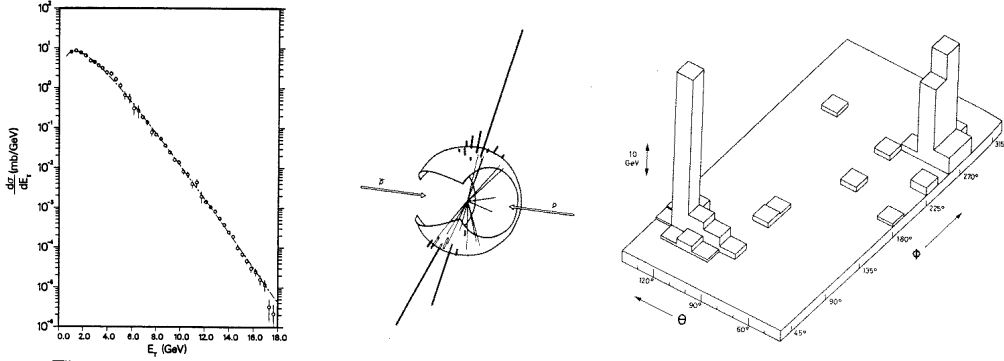


Figure 19: a)(left) NA5 structureless E_T distribution [102]. b,c) UA2 jet event from 1982 ICHEP [103]: b)(center) event shown in geometry of detector; c)(right) “Lego” plot of energy in calorimeter cell as a function of angular position of cell in polar (θ) and azimuthal (Φ) angle space.

skepticism about jets in hadron collisions, particularly in the USA. A ‘phase change’ in belief-in-jets was produced by one UA2 event at the 1982 ICHEP in Paris [103], which, together with the first direct measurement of the QCD constituent-scattering angular distribution, $\Sigma^{ab}(\cos \theta^*)$ (Eq. 7.5), using two-particle correlations, presented at the same meeting (Fig. 20) [103, 104], gave universal credibility to the pQCD description of high p_T hadron physics [105, 91, 106]. Since that time, QCD and jets have become the standard tools of High Energy Physics.

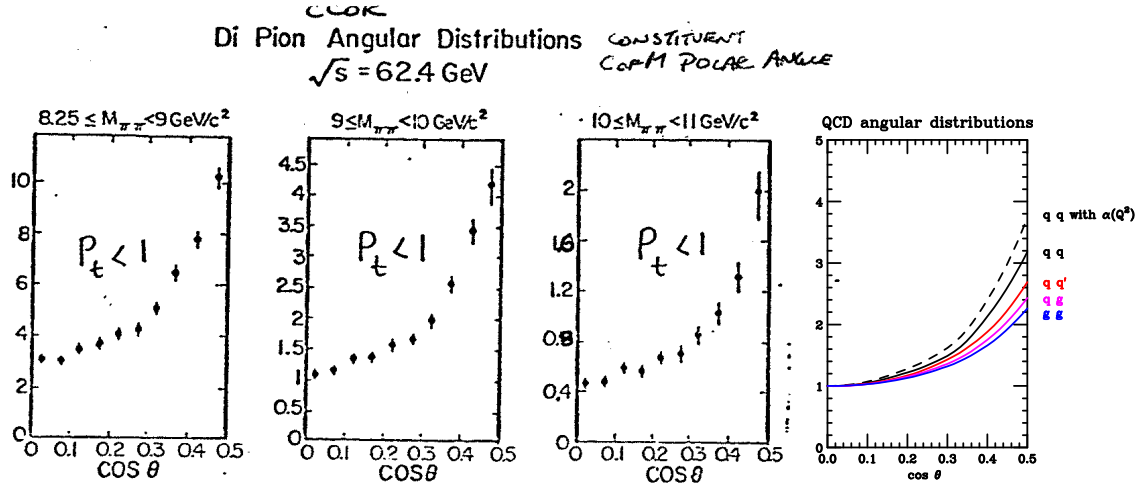


Figure 20: a) (left 3 panels) CCOR measurement [103, 104] of polar angular distributions of π^0 pairs with net $p_T < 1 \text{ GeV}/c$ at mid-rapidity in p-p collisions with $\sqrt{s} = 62.4 \text{ GeV}$ for 3 different values of $\pi\pi$ invariant mass $M_{\pi\pi}$. b) (rightmost panel) QCD predictions for $\Sigma^{ab}(\cos \theta^*)$ for the elastic scattering of gg , qg , qq' , qq , and qq with $\alpha_s(Q^2)$ evolution.

As a final note, recall that hard-scattering is visible by a break in the exponential single particle inclusive spectrum after roughly 3 orders of magnitude in cross section (Fig. 12). However, finding jet structure in E_T distributions measured in 4π calorimeters is much more difficult because the jets are only visible by a break in the E_T spectrum after 5-7 orders of magnitude of cross section (Fig. 21) [76, 75], since the E_T spectrum is even more dominated by soft physics than the single particle spectrum.

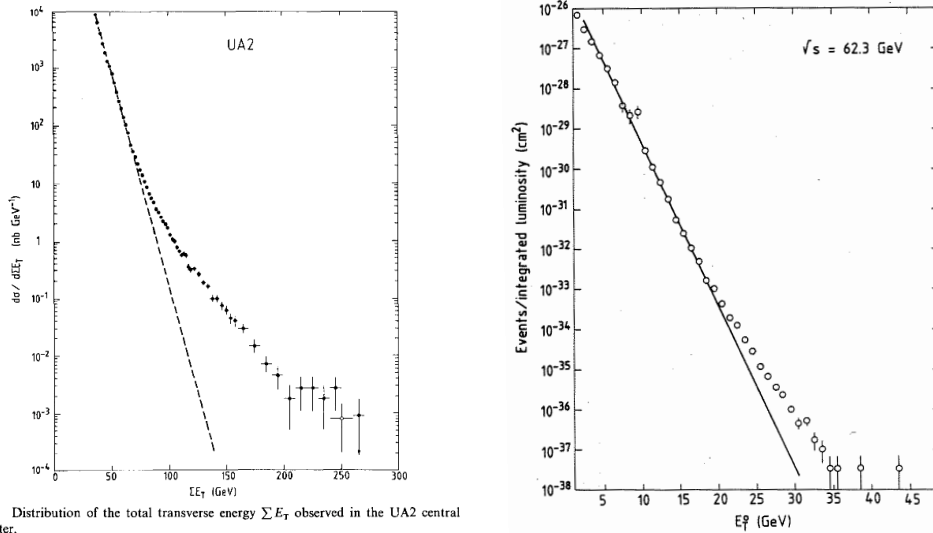


Figure 2 Distribution of the total transverse energy ΣE_T observed in the UA2 central calorimeter.

Figure 21: E_T measurements by: a)(left) UA2 in p- \bar{p} collisions at $\sqrt{s} = 540 \text{ GeV}$ [76]; b)(right) CCOR in p-p collisions at $\sqrt{s} = 62.3 \text{ GeV}$ [75]. The lines indicate extrapolation of the nearly exponential spectrum at lower E_T .

7.5 Status of theory and experiment, circa 1982

Hard-scattering was visible both at ISR and FNAL (Fixed Target) energies via inclusive single particle production at large $p_T \geq 2\text{--}3 \text{ GeV}/c$. Scaling and dimensional arguments for plotting data revealed the systematics and underlying physics. The theorists had the basic underlying physics correct; but many important details remained to be worked out, several by experiment. The transverse momentum imbalance of outgoing parton-pairs, the “ k_T -effect”, was discovered by experiment [89, 95], and clarified by Feynman, Field and Fox [90]. The first modern QCD calculation and prediction for high p_T single particle inclusive cross sections, including non-scaling and the k_T effect was done in 1978, by Jeff Owens and collaborators [96] closely followed and corroborated by Feynman and collaborators [97], under the assumption that high p_T particles are produced from states with two roughly back-to-back jets which are the result of scattering of constituents of the nucleons (partons). The overall $p + p$ hard-scattering cross section in “leading logarithm” pQCD is the sum over parton reactions $a + b \rightarrow c + d$ (e.g. $g + q \rightarrow g + q$) at parton-parton center-of-mass (c.m.) energy $\sqrt{\hat{s}} = \sqrt{x_1 x_2 s}$.

$$\frac{d^3\sigma}{dx_1 dx_2 d\cos\theta^*} = \frac{sd^3\sigma}{d\hat{s} d\hat{y} d\cos\theta^*} = \frac{1}{s} \sum_{ab} f_a(x_1) f_b(x_2) \frac{\pi\alpha_s^2(Q^2)}{2x_1 x_2} \Sigma^{ab}(\cos\theta^*) \quad (7.5)$$

where $f_a(x_1)$, $f_b(x_2)$, are parton distribution functions, the differential probabilities for partons a and b to carry momentum fractions x_1 and x_2 of their respective protons (e.g. $u(x_2)$), and where θ^* is the scattering angle in the parton-parton c.m. system. The parton-parton c.m. energy squared is $\hat{s} = x_1 x_2 s$, where \sqrt{s} is the c.m. energy of the p-p collision. The parton-parton c.m. system moves with rapidity $\hat{y} = (1/2) \ln(x_1/x_2)$ in the p-p c.m. system. Equation 7.5 gives the p_T spectrum of outgoing parton c , which then fragments into a jet of hadrons, including e.g. π^0 . The fragmentation function $D_c^{\pi^0}(z)$ is the probability for a π^0 to carry a fraction $z = p^{\pi^0}/p^c$ of the momentum of outgoing parton c . Equation 7.5 must be summed over all subprocesses leading to a π^0 in the final state weighted by their respective fragmentation functions. In this formulation, $f_a(x_1)$, $f_b(x_2)$ and $D_c^{\pi^0}(z)$ represent the “long-distance phenomena” to be determined by experiment; while the characteristic subprocess angular distributions, $\Sigma^{ab}(\cos\theta^*)$, and the coupling constant, $\alpha_s(Q^2) = \frac{12\pi}{25} \ln(Q^2/\Lambda^2)$, are fundamental predictions of QCD [98, 99].

8. Hard-Scattering at RHIC

For the past decade the single and two-particle techniques developed in the period 1972–1982, largely at the CERN-ISR were used exclusively at RHIC to study hard-scattering in p-p A+A collisions, with outstanding results.

8.1 Single particle (semi-) inclusive measurements

The p-p single particle inclusive p_T spectra measurements in Fig. 22 clearly illustrate the importance of particle identification since all the different particles have different systematic behavior. PHENIX concentrates on mesons and photons since they provide the main backgrounds to lepton and photon searches for which we built this specialized detector, while STAR concentrates on hyperons. Also, inclusive single particle measurements have very precise $\sim 1\%$ p_T scales in contrast

to jets. As shown in Fig. 22b for p-p collisions, jets are excellent if you can do it because they give the best rates. My favorite jet measurement is a search for parity violation in 100 GeV jets to look for quark substructure [107]. Fig. 22a, on a semi-log scale, emphasizes measurements at the lowest p_T including the soft-physics range and the transition to hard-scattering, while the log-log scale on Fig. 22b emphasizes the power-law behavior at high p_T . It is interesting to note that the π^0 and jet spectra are parallel to each other (the same p_T^n dependence, see Eq. 8.3 below), while the direct γ are flatter, corresponding to an n_{eff} closer to 4 on an x_T scaling plot. There should be a simple explanation, but I don't know it.

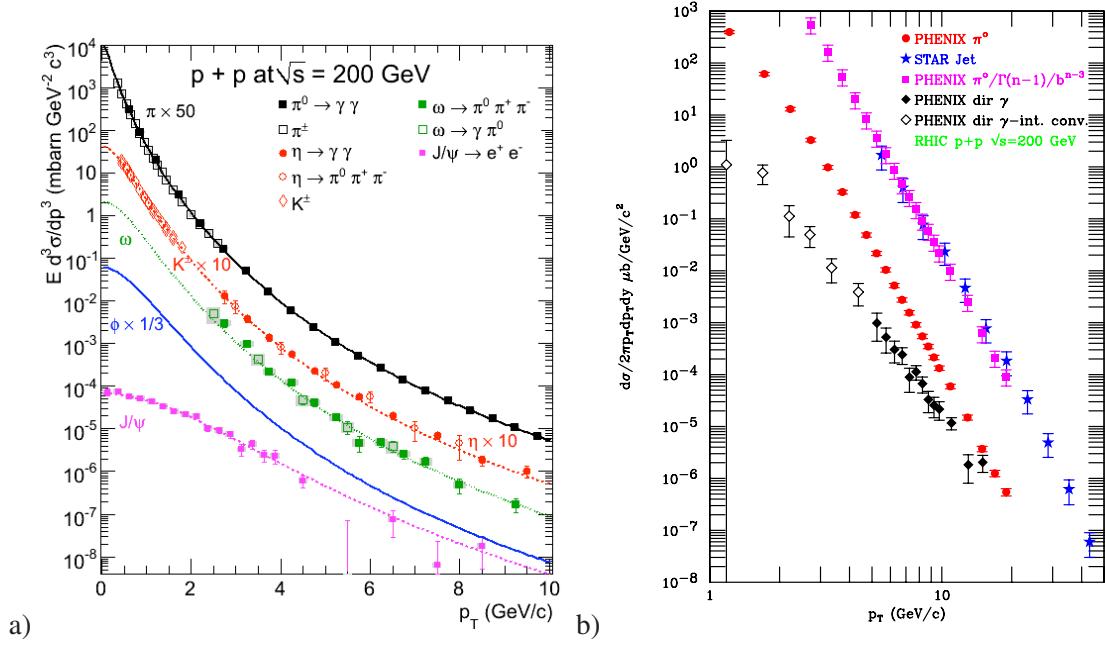


Figure 22: PHENIX p_T invariant cross section at mid-rapidity in p-p collisions at $\sqrt{s} = 200$ GeV. a) Compilation of mesons needed for understanding leptonic background [108] b) Direct- γ [109, 110], π^0 [64] and STAR Jets [111] for hard-scattering studies.

8.1.1 High p_T suppression in Au+Au collisions

One of the major, if not the major discovery at RHIC is the huge suppression of particle production at large p_T in A+A collisions. So far this appears to be consistent with the QCD predictions of energy loss or absorption of the outgoing hard-scattered color-charged partons due to interactions with the presumably deconfined and thus color-charged medium (a liquid version of the QGP) produced in central A+A collisions at RHIC [112]. The suppression is represented by the nuclear modification factor, the ratio R_{AA} of the measured semi-inclusive yield (e.g of π) for a given centrality class to the p-p cross section scaled by $\langle T_{AA} \rangle$ the average overlap integral of the nuclear thickness functions for that centrality class (Eq. 8.1). For pure point-like hard-scattering, $R_{AA} = 1$.

$$R_{AA} = \frac{d^2 N_{AA}^\pi / p_T dp_T dy N_{AA}^{\text{inel}}}{\langle T_{AB} \rangle \times d^2 \sigma_{pp}^\pi / p_T dp_T dy} \quad (8.1)$$

The striking differences of $R_{AA}(p_T)$ in central Au+Au collisions for the many particles measured by PHENIX at RHIC (Fig. 23) illustrates the importance of particle identification for understanding the physics of the medium produced at RHIC. For the entire region $p_T < 20$ GeV/c so far measured

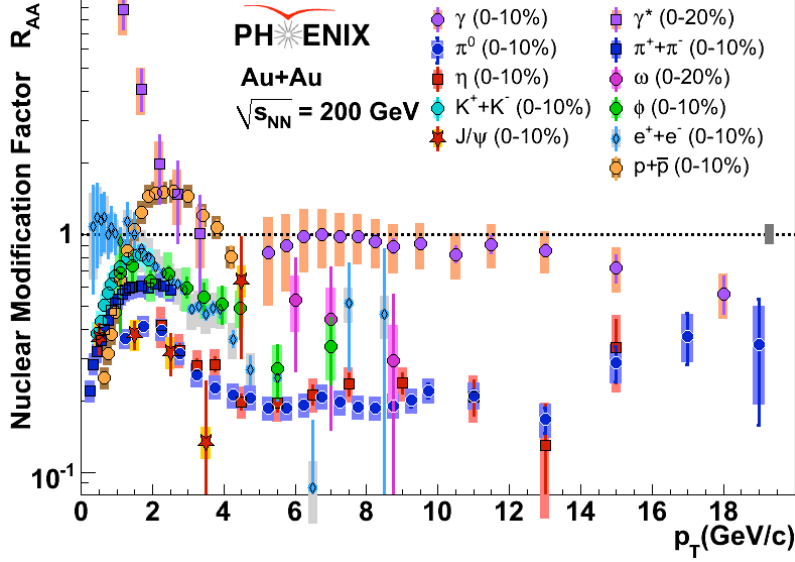


Figure 23: R_{AA} compilation from PHENIX for central Au+Au collisions. With the exception of the direct- γ internal-conversion data (γ^*) for $p_T < 4$ GeV/c where a fit to the p-p data (which is not exponential) is used, all the other values of R_{AA} are computed from the measured Au+Au and p-p p_T spectra.

at RHIC, all particles show suppression for $p_T > 3$ GeV/c with the exception of $p + \bar{p}$, which are enhanced in the region $2 \leq p_T \leq 4$ GeV/c (the “baryon anomaly” [113]), and the direct γ , which are not suppressed, presumably because the outgoing γ ’s do not interact with the color charged medium. New and truly notably this year is the behavior of R_{AA} of direct- γ for $p_T < 2$ GeV/c [109], which is totally and dramatically different from all other particles, exhibiting an order of magnitude exponential enhancement as $p_T \rightarrow 0$. This exponential enhancement is certainly suggestive of a new production mechanism in central Au+Au collisions different from the conventional soft and hard particle production processes in p-p collisions and its unique behavior is attributed to thermal photon production by many authors (e.g. see citations in reference [114]).

8.2 Two-particle correlations at RHIC

8.2.1 A RHIC discovery—di-hadron correlations do not measure the fragmentation function

The two-particle (di-hadron) correlations as measured at RHIC follow the systematics from previous measurements at the CERN-ISR as already shown in Sec. 7.3. However, we learned something new and important at RHIC [59]—the di-hadron correlation, e.g. π^0 -h, where both hadrons are fragments of jets, does not measure the fragmentation function.

PHENIX [59] attempted to measure the mean net transverse momentum of the di-jet, $\langle p_{T\text{pair}} \rangle = \sqrt{2} \langle k_T \rangle$, in p-p collisions at RHIC, where k_T represents the out-of-plane activity of the hard-scattering [90, 91]. This requires the knowledge of $\langle z_t \rangle$ of the trigger π^0 , which PHENIX attempted to calculate using a fragmentation function derived from the measured x_E distributions (Fig. 24a).

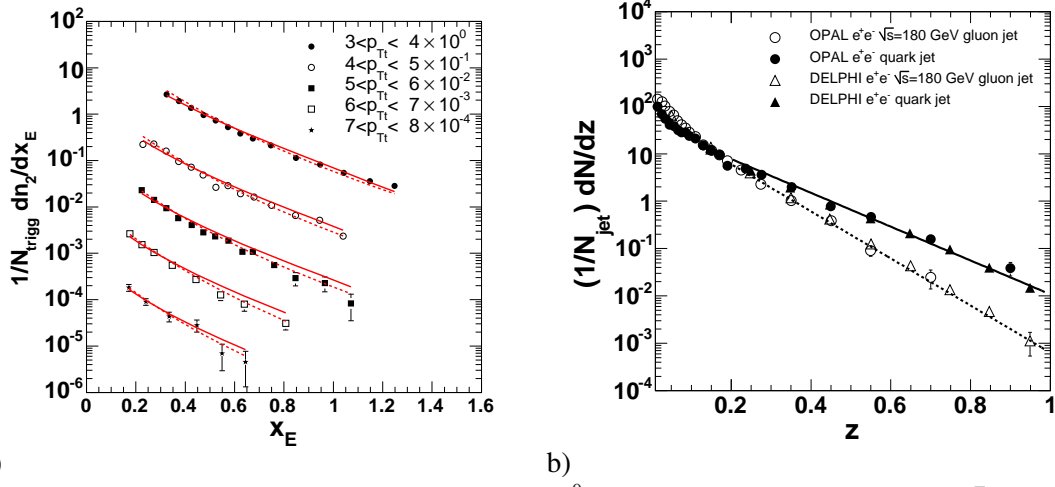


Figure 24: a) x_E distributions from PHENIX [59] for π^0 -h correlations in p-p collisions at $\sqrt{s} = 200$ GeV for several values of p_{T_i} . The solid and dashed lines represent calculations of the distribution for quark (solid lines) and gluon (dashed lines) fragmentation functions based on exponential fits to the LEP measurements [115, 116] shown in b). See Ref. [59] for details

It didn't work. Finally, it was found that starting with either the quark $\approx \exp(-8.2 \cdot z)$ or the gluon $\approx \exp(-11.4 \cdot z)$ fragmentation functions from LEP (Fig. 24b solid and dotted lines), which are quite different in shape, the results obtained for the x_E distributions (solid and dotted lines on Fig. 24a) do not differ significantly! Although nobody had noticed this for nearly 30 years, the reason turned out to be quite simple. The integration over z_t of the trigger jet for fixed trigger particle p_{T_i} is actually an integral over the trigger jet \hat{p}_{T_i} . However since the trigger and away-jets are always roughly equal and opposite in transverse momentum, integrating over \hat{p}_{T_i} simultaneously integrates over \hat{p}_{T_a} and thus also integrates over z of the away-jet.

With no assumptions other than a power law for the jet \hat{p}_{T_i} distribution ($d\sigma_q/\hat{p}_{T_i} d\hat{p}_{T_i} = A\hat{p}_{T_i}^{-n}$), an exponential fragmentation function ($D_q^\pi(z) = Be^{-bz}$), and constant \hat{x}_h , for fixed p_{T_i} as a function of p_{T_a} , it was possible to derive the x_E distribution in the collinear limit, where $p_{T_a} = x_E p_{T_i}$ [59]:

$$\left. \frac{dP_\pi}{dx_E} \right|_{p_{T_i}} \approx N(n-1) \frac{1}{\hat{x}_h} \frac{1}{(1 + \frac{x_E}{\hat{x}_h})^n}, \quad (8.2)$$

and $N = \langle m \rangle$ is the multiplicity of the unbiased away-jet. The shape of the x_E distribution (Fig. 24a) is given by the power n of the partonic and inclusive single particle invariant transverse momentum spectra and does not depend on the exponential slope of the fragmentation function (Fig. 24b). Note that Eq. 8.2 provides a relationship between the ratio of the away and trigger particle's transverse momenta, $x_E \approx p_{T_a}/p_{T_i}$, which is measured, to the ratio of the transverse momenta of the away and trigger jets, $\hat{x}_h = \hat{p}_{T_a}/\hat{p}_{T_i}$, which can thus be deduced. In p-p collisions the imbalance of the away-jet and the trigger jet ($\hat{x}_h \sim 0.7 - 0.8$) is caused by k_T -smearing [90, 59]. In A+A collisions, \hat{x}_h is sensitive to the relative energy loss of the trigger and associated jets in the medium, which can thus be measured [85].

The same derivation gives a simple formula for Bjorken's parent-child ratio, the ratio of the

number of π at a given p_{T_i} to the number of partons(q) at the same p_{T_i} :

$$\left. \frac{\pi^0}{q} \right|_{\pi^0} (p_{T_i}) \approx \frac{\Gamma(n-1)}{b^{n-3}} \quad (8.3)$$

I used Eq. 8.3 together with a half and half mixture of quark and gluon jets with $b_q = 8.2$ $b_g = 11.7$ from Fig. 24b to obtain the parton cross section from the π^0 cross section on Fig. 22b [117].

8.2.2 Two-particle correlations in A+A collisions are much more complicated than for p-p

In analogy to Fig. 18 (above), the di-hadron correlations in Au+Au collisions (Fig. 25) show a di-jet structure. However, one of the many interesting new features in Au+Au collisions is that

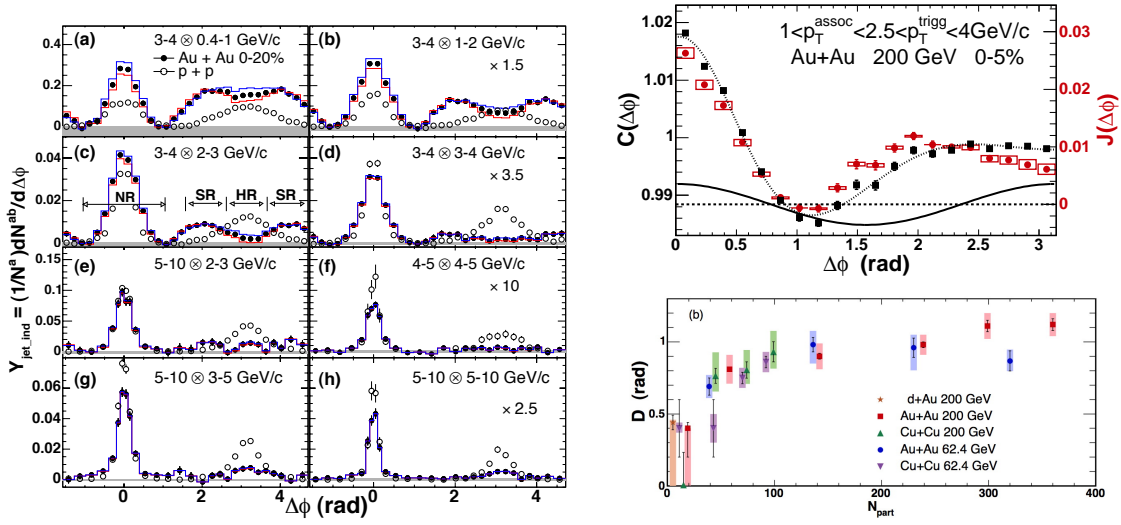


Figure 25: a-h) (left) PHENIX [118] azimuthal correlation conditional yield of associated h^\pm particles with p_T^b for trigger h^\pm with p_T^a for the various $p_T^a \otimes p_T^b$ combinations shown. i) (right)-(top) PHENIX [119] azimuthal correlation function $C(\Delta\phi)$ of h^\pm with $1 \leq p_{T_a} \leq 2.5$ GeV/c with respect to a trigger h^\pm with $2.5 \leq p_{T_i} \leq 4$ GeV/c in Au+Au central collisions, where the line with data points indicates $C(\Delta\phi)$ before correction for the azimuthally modulated (v_2) background, and the other line is the v_2 correction which is subtracted to give the jet correlation function $J(\Delta\phi)$ (data points). j) (right)-(bottom) PHENIX D parameters [119], the angular distance of the apparently displaced peak of the $J(\Delta\phi)$ distribution from the angle $\Delta\phi = \pi$ as a function of centrality, represented as the number of participants N_{part} , for the systems and c.m. energies indicated.

the away side azimuthal jet-like correlations (Fig. 25c) are much wider than in p-p collisions and show a two-lobed structure (“the shoulder” (SR)) at lower p_{T_i} with a dip at 180° , reverting to the more conventional structure of a peak at 180° (“the head” (HR)) for larger p_{T_i} . The wide away-side correlation in central Au+Au collisions is further complicated by the large multiparticle background which is modulated in azimuth by the v_2 collective flow of a comparable width to the jet correlation (Fig. 25i). After the v_2 correction, the double peak structure $\sim \pm 1$ radian from π , with a dip at π radians, becomes evident. The double-peak structure may indicate a reaction of the medium to a passing parton in analogy to a “sonic boom” or the wake of a boat and is under active

study both theoretically [120] and experimentally. PHENIX characterizes this effect by the half-width D (~ 1.1 radian) of the Jet function, $J(\Delta\phi)$, the angular distance of the displaced peak of the distribution from the angle $\Delta\phi = \pi$. One of the striking features of the wide away side correlation is that the width D (Fig. 25j) does not depend on centrality, angle to the reaction plane, p_{T_a} and $\sqrt{s_{NN}}$, which seems problematic to me if the effect is due to a reaction to the medium.

As discussed above, the x_E (also denoted z_T) distribution from di-hadron collisions does not measure the fragmentation function. Instead, it is sensitive to the ratio of the away parton transverse momentum to the trigger parton transverse momentum, $\hat{x}_h = \hat{p}_{T_a}/\hat{p}_{T_t}$, which is a measure of the differential energy loss of the away parton relative to the trigger parton which is surface biased due to the steeply falling \hat{p}_{T_t} spectrum [121, 122]. The energy loss of the away-parton is indicated by the fact that the x_E distribution in Au+Au central collisions e.g. for $4 \leq p_{T_t} \leq 5$ GeV/c (Fig. 26a) from the data in Fig. 25 [118] is steeper than that from p-p collisions. Eq. 8.2 provides excellent fits to these distributions in both p-p and Au+Au collisions (Fig. 26a), where fits to the full away side azimuth Head + Shoulder (HS) region are shown. In p-p collisions, the imbalance of the away-

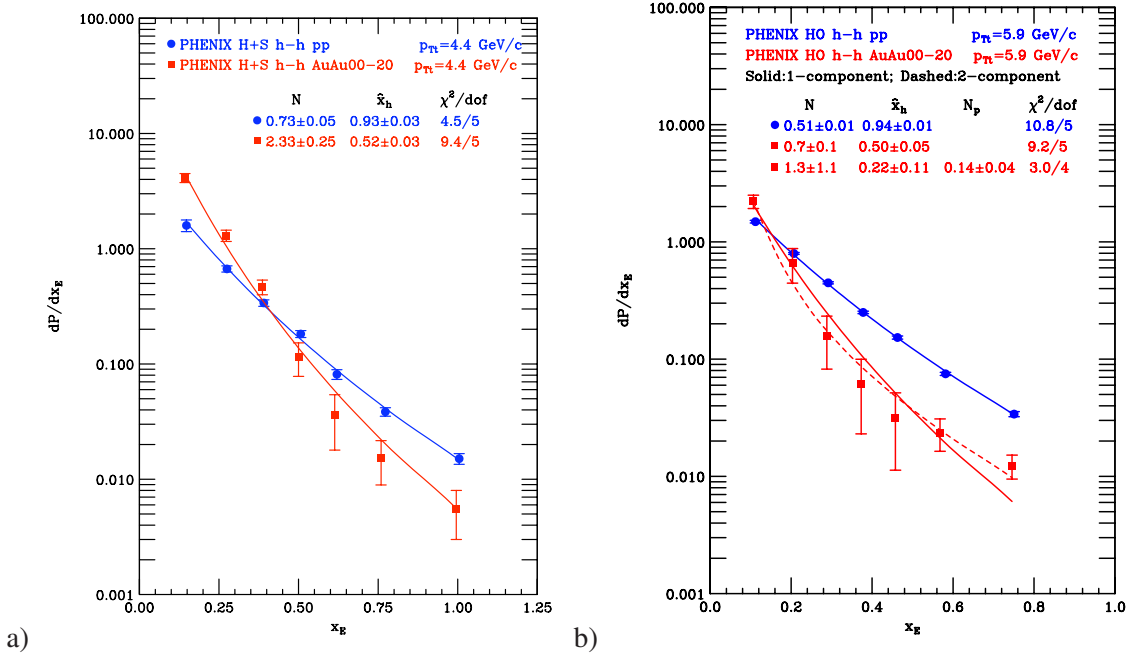


Figure 26: a) x_E distribution [118] dP/dx_E of associated h^\pm per trigger h^\pm with $4 \leq p_{T_t} \leq 5$ GeV/c for the full away side azimuth, $|\Delta\phi - \pi| < \pi/2$, in p-p (circles) and Au+Au central (0-20%) collisions (squares). Fits to Eq. 8.2 are shown with best-fit parameters indicated. b) Same plot for $5 \leq p_{T_t} \leq 10$ GeV/c data [118], for the Head region only (HO), $|\Delta\phi - \pi| < \pi/6$.

parton and the trigger parton indicated by the fitted value of $\hat{x}_h = 0.93 \pm 0.03$ in Fig. 26a is caused by k_T -smearing. In A+A collisions, the fitted value $\hat{x}_h = 0.52 \pm 0.03$ indicates that the away parton has lost energy relative to the trigger parton.

For larger p_{T_t} , another interesting effect takes place, punch-through of narrow away-side peaks consistent with roughly the same azimuthal width and x_E distributions as in p-p collisions [122]. Fig. 26b shows the x_E distributions and fits at higher $5 \leq p_{T_t} \leq 10$ GeV/c where the region of

integration of the away-side azimuthal distribution has been restricted to the head-region only (HO) in both p-p and Au+Au collisions. The fitted values of \hat{x}_h are nearly identical in Fig. 26b ($\hat{x}_h = 0.94 \pm 0.01$ in p-p and $\hat{x}_h = 0.50 \pm 0.05$) and Fig. 26a but the integrated away-side multiplicity N is reduced in the HO region compared to the full-away side (HS). Of more importance to note is that the fit to the Au+Au HO data (Fig. 26b) is greatly improved ($\Delta\chi^2 = 6.2/1$) if a second component with the same \hat{x}_h as the p-p distribution is added (dashed-curve), statistically indicating a parton that has apparently punched through the medium without losing energy. The two-component fit shows 27% punch-through and a much larger energy loss, 77%. This is more clearly exhibited by taking the ratio, I_{AA} of the x_E distributions for Au+Au to p-p (Fig. 27a), and is evident directly in the STAR z_T (same as x_E) distribution [123] (Fig. 27b) by the sharp change in slope at z_T (x_E) = 0.5 in Au+Au for $6 < p_{T_i} < 10$ GeV/c.

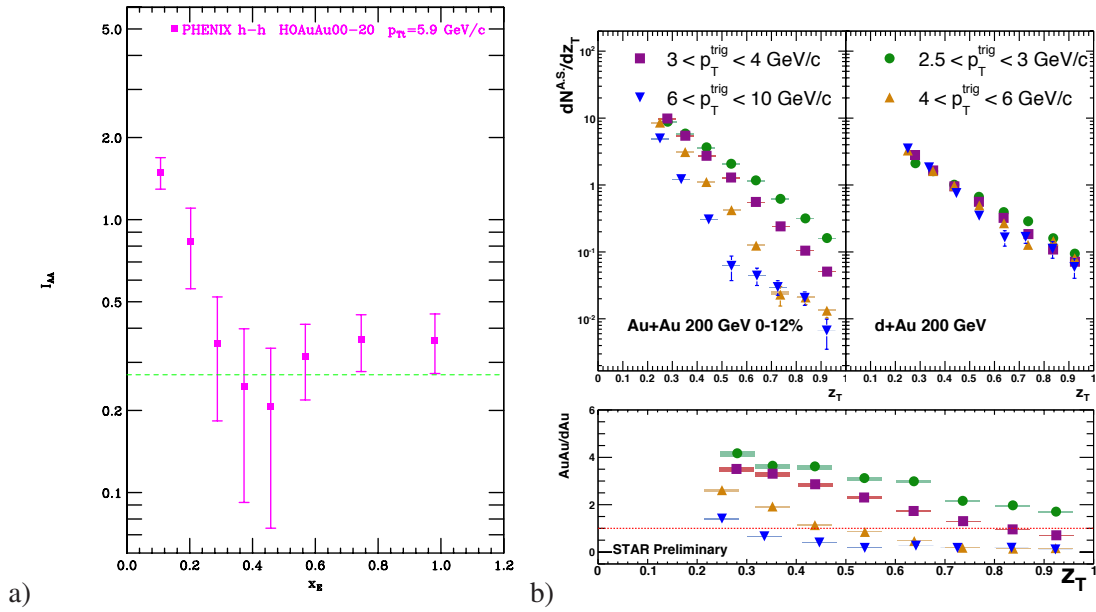


Figure 27: a) $I_{AA}(x_E)$ from the ratio of Au+Au/pp distributions in Fig. 26b. Dashed line is 27% punch-through from fit. b) STAR [123] away side z_T (same as x_E) distributions for various p_{T_i} in Au+Au, d+Au and their ratio in $\sqrt{s_{NN}} = 200$ GeV collisions.

The punch-through and normal fragmentation of partons which have lost energy are standard features of the QCD energy loss models. For instance the ZOWW [124] model breaks down the away-side fragmentation function to:

$$D_{h/c}(z_c, \Delta E_c, \mu^2) = (1 - e^{-(L/\lambda)}) \left[\frac{z'_c}{z_c} D_{h/c}^0(z'_c, \mu^2) + \left\langle \frac{L}{\lambda} \right\rangle \frac{z'_g}{z_c} D_{h/g}^0(z'_g, \mu^2) \right] + e^{-(L/\lambda)} D_{h/c}^0(z_c, \mu^2), \quad (1)$$

where $z'_c = p_T/(p_{Tc} - \Delta E_c)$, $z'_g = \langle L/\lambda \rangle p_T/\Delta E_c$ are the rescaled momentum fractions, ΔE_c is the average radiative parton energy loss and $\langle L/\lambda \rangle$ is the number of scatterings.

In words, the three terms in the above equation correspond to normal fragmentation of partons which have lost energy; the fragmentation of the lost energy, assumed to be a gluon; normal fragmentation with full original energy of punch-through partons. This ‘paradigm’ is consistent, as far as I can tell, with all measured $I_{AA}(x_E)$ distributions in di-hadron correlations (Fig. 27)—an exponential decrease at low x_E from energy-loss and a flat distribution at large x_E due to punch-through when no radiation occurs.

The discrete radiation of relatively large energy gluons is characteristic of the LPM effect [49, 125] in QCD, where in distinction to QED, it is the radiated gluon that interacts coherently with the medium. This suppresses the gluon spectrum for large radiated energy k (rather than at low k as in QED, Fig. 4a) but the coherence comes from gluons with a k larger than some critical value (ω_{BH}) which is relatively hard, 1–4 GeV. Thus if LPM radiation occurs there is a large radiation loss, but there is a Poisson probability $e^{-L/\lambda}$ that no radiation occurs leading to punch-through. However, as I understand it, multiple scattering (p_T broadening), elastic and normal Bethe-Heitler radiative loss should take place even with punch-through, so we still have a long way to go on this issue.

The energy-loss models all do quite well in describing the suppression, $R_{AA}(p_T)$, for single-inclusive π^0 , although each model has different parameters [126]. However, the suppression of direct- e^\pm from heavy quark decays (recall Fig. 23) disfavors radiative models since, naively, heavy quarks should radiate much less than light quarks in the medium. This has attracted much theoretical attention and is still not explained [127, 128].

For two-particle correlations, no clear paradigm has emerged for the two-lobed wide away-jet structure. Some suggestions are:

- Mach or Cerenkov cone due to medium reaction. Since the effect vanishes for larger p_{T_i} , with no dependence on centrality or p_{T_a} (recall Fig. 25j), I find this explanation unlikely. Further studies with particle identification might show whether the composition of the shoulder is the same as the medium or the jet for a given p_{T_a} —kind of like the difference of being hit by the wake (water) or the boat (wood).
- Fluctuations of v_3 [129, 130]: $\langle v_3 \rangle = 0$ at mid-rapidity but $\langle v_3^2 \rangle \neq 0$. This gives the best fits to the azimuthal correlation functions $C(\Delta\phi)$ and the constant value of $D \approx 60^\circ$ (Fig. 25) and is consistent with vanishing at large p_{T_i} . Lots of ongoing work at the present time.
- NLO 3-jet events less suppressed than di-jets due to smaller path-length in medium [131].

9. Direct- γ -h correlations do measure the fragmentation function

Direct single- γ production via the inverse QCD-compton process [132]:

$$g + q \rightarrow \gamma + q \quad (9.1)$$

is an important probe in p-p collisions because it is sensitive the gluon structure function at leading order as well as higher orders [133]. It is possibly even more important in A+A collisions because the γ is a direct participant in the hard-scattering (at the constituent level), which emerges from the medium without interacting and can be measured precisely. This means that, modulo k_T , the p_T of the quark jet which is equal and opposite to that of the direct- γ is known precisely. Furthermore,

since the direct- γ is not a fragment of a jet, but a direct participant in the hard-scattering, this means that the fragmentation function can be measured by the direct- γ -hadron x_E (z_T) distribution, as originally suggested by Wang, Huang and Sarcevic in 1996 [134], ‘the golden channel’ [135].

There are nice reviews of both the theory [105] and the experimental discovery of direct-single- γ production at the CERN-ISR in 1978–80 and other early measurements [136]. Measurements of direct- γ at RHIC in both p-p [137] and Au+Au [138] collisions have shown the absence of suppression for this probe which does not interact with the medium (recall Fig. 23). Calculations of direct- γ production in QCD give impressive agreement with the data over a wide range of c.m. energies [133]. Other nice features of direct- γ production from the inverse QCD-compton effect (Eq. 9.1) is that the γ are isolated and the away-jet is a quark-jet, 8 times more likely u than d .

Beyond Leading Order, single- γ may be produced in the fragmentation process [105]; but these γ are not isolated. However, measurements of $\gamma-h$ azimuthal correlations in p-p collisions at both the CERN-ISR [139] and RHIC [140] (Fig. 28) show that direct- γ are isolated, with very few, if any, accompanying same-side particles, while π^0 have accompanying particles since they are fragments of jets from high p_T partons. This is strong evidence against a significant fragmentation component for direct- γ production, easily $\lesssim 10\%$.

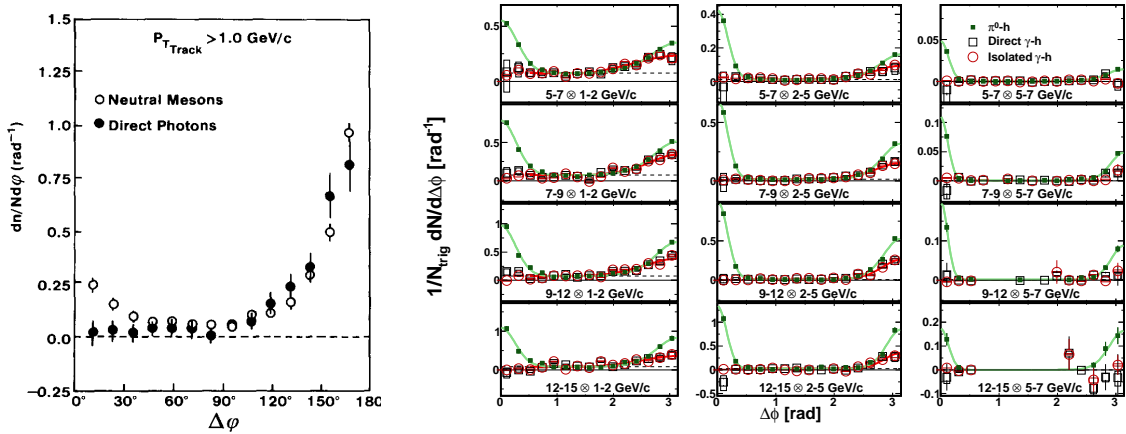


Figure 28: Direct single- γ -h and π^0 -h azimuthal correlations in p-p collisions: a) $\sqrt{s_{NN}} = 62.4$ GeV, $p_{T_i} > 6$ GeV/c [139]; b) $\sqrt{s} = 200$ GeV, p_{T_i} , p_{T_a} as indicated [140].

The x_E and p_{out} distributions in p-p collisions from π^0 -h and direct- γ -h correlations from new data at RHIC [140] are shown in Fig. 29. For these measurements of direct- γ -h correlations, an isolation cut has been made to improve the systematic uncertainty in subtracting the background from π^0 -h correlations. The x_E distributions show a flatter slope of the π^0 -h distribution compared to the direct- γ -h distribution, as discussed for Fig. 18d (which is for jet-h vs π^0 -h correlations) [90], showing that the γ plays the expected role of a jet for correlation measurements, albeit with a much higher precision measurement of p_T and a much lower rate. Of course, the x_E distribution from the isolated-direct- γ -h measurement is actually the fragmentation function. The p_{out} distributions for π^0 -h and isolated-direct- γ -h correlations (Fig. 29) appear to be nearly identical and both show the features of a Gaussian distribution for $p_{out} < 3$ GeV/c, which is the k_T effect, now thought to be due to resummation of soft gluons [133], and a power-law tail from NLO hard-gluon emission. This

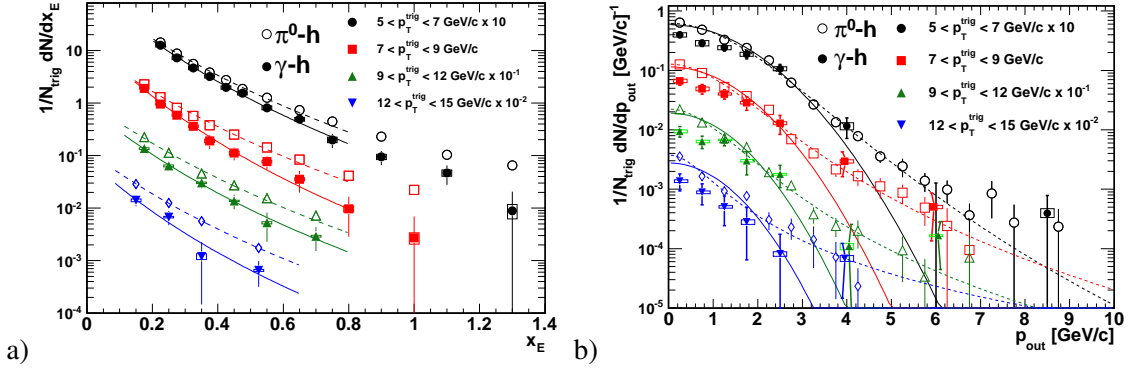


Figure 29: a) x_E and b) p_{out} distributions from π^0 -h and isolated direct- γ -h correlations [140]

is the first time that the k_T effect has been measured with direct- γ ; and the $\sqrt{\langle k_T^2 \rangle}$ is essentially identical in π^0 and direct- γ production.

9.1 The fragmentation function in p-p collisions

From the discussion above, the x_E (z_T) distribution for direct- γ -h (Fig. 29a) should be a measurement of the u quark fragmentation function. To make this more apparent, we follow the approach of Borghini and Wiedemann (Fig. 30a) [141] who proposed using the hump-backed or $\xi = \ln(1/z)$ distribution of jet fragments, which is a signature of QCD coherence [142] for small

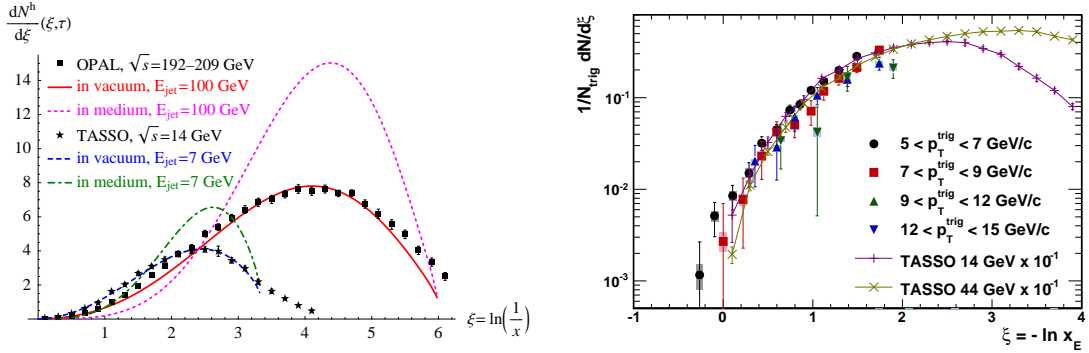


Figure 30: a) Predicted ξ distributions in vacuum and in medium for two jet energies [141], together with measurements from e^+e^- collisions [143, 115] b) $\xi = \ln 1/x_E$ distributions for PHENIX isolated direct- γ data for all p_{T_i} ranges combined, compared to e^+e^- collisions at $\sqrt{s} = 14$ and 44 GeV [143].

values of particle momentum fraction, $z = p/E_{jet}$, to explore the medium-modification of jets in heavy ion collisions. The use of the ξ variable would emphasize the increase in the emission of fragments at small z due to the medium induced depletion of the number of fragments at large z . The jet energy must be known for this measurement so that it was presumed that full jet reconstruction would be required. However, the direct- γ -h correlation is (apart from the low rate) actually better for this measurement since both the energy and identity of the jet (8/1 u -quark, maybe 8/2 if the $\bar{q} + q \rightarrow \gamma + g$ channel is included) are known to high precision. The PHENIX x_E distributions

(Fig. 29a) converted to the ξ distributions are shown in Fig. 30b in quite excellent agreement with the dominant u -quark fragmentation functions measured in e^+e^- collisions at $\sqrt{s}/2 = 7$ and 22 GeV [143], which cover a comparable range in jet energy. Also, Fig. 30b is plotted on a log scale for $dN/d\xi$ which allows the full range of the fragmentation function, notably for $z > 0.2$, $\xi < 1.6$ to be visible.

9.2 “The golden channel”, direct- γ -h in Au+Au collisions

Before discussing direct- γ -h correlations in Au+Au collisions, it is worth reviewing the results for π^0 -h correlations, presented in Fig. 31 [144] as I_{AA} , the ratio of the p_T distributions of the partner-h in Au+Au central collisions to p-p collisions, for several values of trigger π^0 p_{T_i} at $\sqrt{s_{NN}} = 200$ GeV. All the distributions show the characteristic shape of an exponentially falling I_{AA}

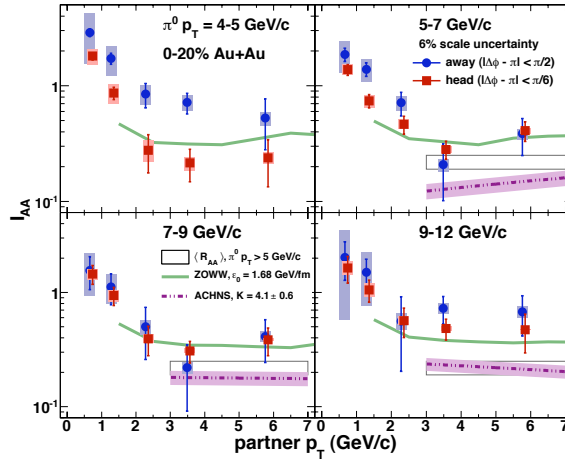


Figure 31: a) PHENIX [144] Away-side I_{AA} for a “head-only” (HO) $|\Delta\phi - \pi| < \pi/6$ selection (solid squares) and the entire away-side (H+S), $|\Delta\phi - \pi| < \pi/2$ (solid circles) as a function of partner-h p_T for various p_{T_i} . Calculations from two different predictions are shown for the head region in applicable partner-h p_T ranges. $R_{AA}(p_T)$ of π^0 for $p_{T_i} > 5$ GeV/c [145] are included for comparison.

for lower values of p_{T_a} due to energy loss of the away-jet and a flat distribution for larger values of p_{T_a} due to partons that punch-through the medium with no energy loss and then fragment normally as in p-p collisions. Two other important points are evident from Fig. 31: a) the H+S and HO data become the same for $p_{T_i} > 7$ GeV/c because the away-jets in Au+Au are no longer anomalously wide and are consistent with the shape of the p-p azimuthal correlation in both the falling and flat part of the distribution; b) In the punch-thru region, $I_{AA} > R_{AA}$ at the same value of p_T .

The expectations for the difference in behavior of π^0 -h and direct- γ -h correlations for the cases of either a totally absorbing medium (surface emission only) and a translucent lossy medium (partons can emerge from the medium having lost energy) are briefly summarized:

Totally absorbing medium:

direct- γ -h: γ emerge from all throughout the medium. Away partons are either totally absorbed or emitted from the surface with normal fragmentation, same surface bias as for inclusive hadrons (but on the away surface). $I_{AA}(p_{T_i}) = \text{constant} = \text{fraction not absorbed} = R_{AA}^h(p_{T_i})$.

π^0 -h: For inclusive hadrons, strong surface bias: only partons emitted from the surface are seen. For di-hadrons, only tangential emission is seen. $I_{AA} = \text{constant} = \text{the fraction of surface emission that is tangent to the surface}$. Therefore $I_{AA} < R_{AA}(h)$.

Translucent lossy medium:

direct- γ -h: Away partons lose energy. Some punch through or are tangent. I_{AA} is exponentially decreasing at small x_E due to partons with energy loss, constant at larger x_E due to punch-thru.

π^0 -h: Roughly the same except away partons may lose more energy due to surface bias of the trigger, and fewer may punch through.

The π^0 -h data in Fig. 31 show $I_{AA} > R_{AA}$ so disfavor the totally absorbing medium. The present direct- γ -h data are less conclusive.

Fig. 32a shows the PHENIX preliminary x_E (z_T) distributions for direct- γ -h correlations in p-p and Au+Au from QM2009 [146]. The p-p data show nice x_E scaling for all p_{T_i} (as would be expected for a fragmentation function) and are fit to an exponential, e^{-bz_T} , with slope $b = 6.89 \pm 0.64$. The Au+Au data also exhibit reasonable x_E scaling for all p_{T_i} with an exponential slope $b = 9.49 \pm 1.37$. The x_E scaling and steeper slope in Au+Au suggest a constant fractional energy loss of the away-side parton; but the statistical significance is marginal. The thin red line shows that possibly $b \rightarrow 6.89$ for $z_T > 0.4$ which would imply $I_{AA} = \text{constant}$ for $x_E > 0.4$ as for π^0 -h. The STAR [147] measurement of π^0 -h and direct- γ -h I_{AA} as a function of z_T for $8 < p_{T_i} < 16$ GeV/c are shown in Fig. 32b and show equal and constant $I_{AA} \simeq 0.3$ for $0.3 \leq z_T \leq 0.9$ for both the π^0 -h and direct- γ correlations. There is no evidence in either case for an exponential rise of I_{AA} towards $z_T = 0$, possibly because the $z_T > 0.3$ range is too high. Also the STAR value of $I_{AA} \simeq 0.3$ for π^0 -h is smaller than the PHENIX value, $I_{AA} = 0.50 \pm 0.08$, in the same p_{T_i} range.

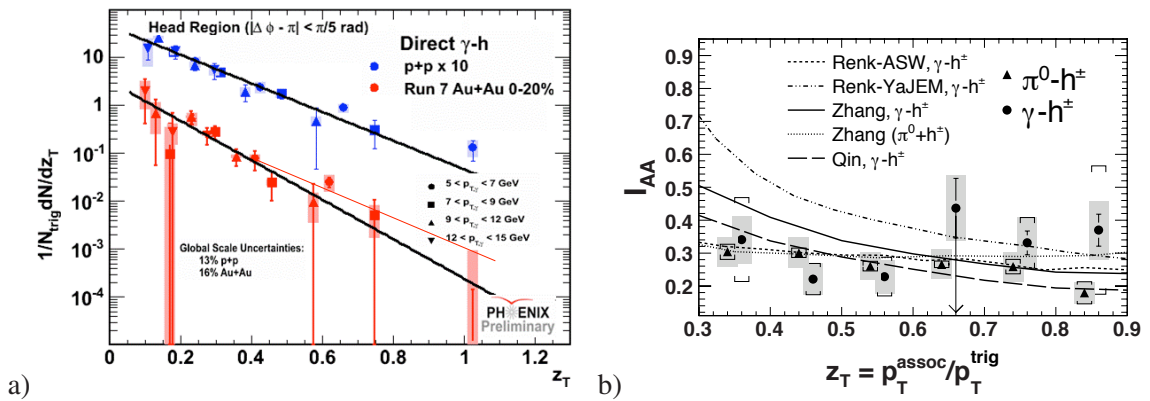


Figure 32: a) PHENIX [146] preliminary z_T (x_E) distribution ($|\Delta\phi - \pi| < \pi/6$) for direct- γ -h, in Au+Au (red), and multiplied by a factor of 10 for p-p (blue), at $\sqrt{s_{NN}} = 200$ GeV. b) STAR [147] away-side I_{AA} vs. z_T for π^0 -h (triangles) and direct- γ -h (circles) with $8 < p_{T_i} < 16$ GeV/c at $\sqrt{s_{NN}} = 200$ GeV. For a discussion of the curves see Refs. [147, 135].

In summary, the results of measurements of the “golden” (but difficult) channel, direct- γ -h, are at too early a stage to tell whether this channel will live up to its promise to understand the QGP, and QCD in a medium; i.e. whether it will be a lasting paradigm, or go the way of the J/ψ .

References

- [1] *The Frontiers of Nuclear Science, NSAC Long Range Plan 2007*.
- [2] J. Dunlop *et al.*, *STAR Beam Use Proposal*, June 2009.
- [3] H. Appelshäuser *et al.* (NA49 Collaboration), *Phys. Lett. B* **459**, 679-686 (1999).
- [4] M. J. Tannenbaum, *Phys. Lett. B* **498**, 29-34 (2001).
- [5] V. Koch, [arXiv:0810.2520v1 \[nucl-th\]](#).
- [6] D. Adamová, *et al.* (CERES Collaboration), *Nucl. Phys. A* **811**, 179-196 (2008).
- [7] C. Amsler *et al.* (Particle Data Group), *Phys. Lett. B* **667**, 1 (2008).
- [8] For example, see P. Amaral *et al.* (ATLAS TileCal Collaboration), *Eur. Phys. J. C* **20**, 487 (2001).
- [9] P. L. Anthony *et al.*, *Phys. Rev. D* **56**, 1373 (1997).
- [10] G. Diambri-Palazzi, *Rev. Mod. Phys.* **40**, 611 (1968).
- [11] M. J. Tannenbaum, BNL-34614, *Proc. SSC Fixed Target Workshop*, The Woodlands TX, Jan 27-29, 1984, pp 56-61. N.B. this calculation is based on original code from Roy Schwitters. Also, Rolf Baier liked this paper so much, that he requested a preprint.
- [12] T. D. Lee and C. N. Yang, *Phys. Rev. Lett.* **4**, 307–311 (1960).
- [13] M. Schwartz, *Phys. Rev. Lett.* **4**, 307–307 (1960). Also see, B. Pontecorvo, *Sov. Phys. JETP* **10**, 1236–1240 (1960) [*Zh. Eksp. Teor. Fiz.* **37**, 1751-1757 (1959)].
- [14] G. Danby *et al.*, *Phys. Rev. Lett.* **9**, 36–44 (1962).
- [15] T. D. Lee and C. N. Yang, *Phys. Rev.* **119**, 1410–1419 (1960).
- [16] R. Cool *et al.*, *Proc. 12th Int. Conf. High Energy Physics August 5-15* (Moscow: Atomizdat, 1964) v.1 pp 852–856.
- [17] A. Zichichi, *Proc. 12th Int. Conf. High Energy Physics August 5-15* (Moscow: Atomizdat, 1964) v.2 p 35.
- [18] G. Arnison *et al.* (UA1 Collaboration), *Phys. Lett. B* **122**, 102–116 (1983).
- [19] M. Banner *et al.* (UA2 Collaboration), *Phys. Lett. B* **122**, 476–485 (1983).
- [20] J. A. Appel *et al.* (UA2 Collaboration), *Z. Phys. C* **30**, 1–22 (1986).
- [21] J. Alitti *et al.* (UA2 Collaboration), *Phys. Lett. B* **276**, 354–364 (1992).
- [22] See *Bull. Am. Phys. Soc.* **51**, (2010) abstracts from PHENIX p. 193, STAR p. 222.
- [23] For example, see *Proc. Adriatico Research Conf. on Trends in Collider Spin Physics*, Eds. Y. Onel, N. Paver, A. Penzo (World Scientific, Singapore, 1997).
- [24] R. C. Lamb *et al.*, *Phys. Rev. Lett.* **15**, 800–802 (1965).
- [25] R. Burns *et al.*, *Phys. Rev. Lett.* **15**, 830–834 (1965).

- [26] P. J. Wanderer, Jr. *et al.*, *Phys. Rev. Lett.* **23**, 729–733 (1969).
- [27] F. Chilton, A. M. Saperstein and E. Shrauner, *Phys. Rev.* **148**, 1380–1384 (1966).
- [28] Y. Yamaguchi, *Nuovo Cimento* **43**, 193 (1966).
- [29] J. H. Christenson *et al.*, *Phys. Rev. Lett.* **25**, 1523–1526 (1970).
- [30] S. D. Drell and T.-M. Yan, *Phys. Rev. Lett.* **25**, 316–320 (1970).
- [31] G. Altarelli, R. A. Brant and G. Preparata, *Phys. Rev. Lett.* **26**, 42–46 (1971). My familiarity with this paper may be understood by referring to the [following article](#) in the journal.
- [32] J. D. Bjorken, *Phys. Rev.* **179**, 1547–1553 (1969).
- [33] L. M. Lederman *et al.*, [NAL Proposal No. 70, 1970, Study of Lepton Pairs from Proton-Nuclear Interactions: Search for Intermediate Bosons and Lee-Wick Structure](#).
- [34] R. L. Cool *et al.*, [Preliminary Proposal ISRC/69-43, ISR Study of Dileptons](#); B. J. Blumenfeld *et al.*, [CCR Proposal, ISRC/69-43/Add, Search for Massive Dileptons](#).
- [35] J. J. Aubert *et al.*, *Phys. Rev. Lett.* **33**, 1404–1406 (1974).
- [36] J.-E. Augustin *et al.*, *Phys. Rev. Lett.* **33**, 1406–1408 (1974).
- [37] Ch. Peyrou, *J. Phys. Colloques* **43**, C8-7–C8-67 (1982).
- [38] T. Appelquist and H. D. Politzer, *Phys. Rev. Lett.* **34**, 43–45 (1975); A. De Rújula and S. L. Glashow, *Phys. Rev. Lett.* **34**, 46–49 (1975).
- [39] S. W. Herb *et al.* (CFS Collaboration), *Phys. Rev. Lett.* **33**, 1406–1408 (1974).
- [40] J. Badier *et al.* (NA3 Collaboration), *Phys. Lett. B* **86**, 98–102 (1979).
- [41] S. Falciano *et al.* (NA10 Collaboration), *Phys. Lett. B* **158**, 92–96 (1985).
- [42] F. Prino *et al.* (NA50 Collaboration), *Proc. 30th Int. Symposium on Multiparticle Dynamics (ISMD2000)*, Eds T. Csorgo, S. Hegyi, W. Kittel (World Scientific, Singapore, 2001) pp 492–500. [hep-ex/0101052](#).
- [43] M. C. Abreu *et al.* (NA50 Collaboration), *Phys. Lett. B* **450**, 456–466 (1999).
- [44] T. Matsui and H. Satz, *Phys. Lett. B* **178**, 416–422 (1986).
- [45] C. Baglin *et al.* (NA38 Collaboration), *Phys. Lett. B* **220**, 471–478 (1989).
- [46] A. Adare *et al.* (PHENIX Collaboration), *Phys. Rev. Lett.* **98**, 232301 (2007).
- [47] R. Arnaldi *et al.* (NA60 Collaboration), submitted to *Phys. Rev. Lett.*, [arXiv:1004.5523v1](#).
- [48] For example, see discussion in M. J. Tannenbaum, [arXiv:1006.5701v1](#), pp 21–23.
- [49] R. Baier, Yu. L. Dokshitzer, A. H. Mueller, S. Peigné and D. Schiff, *Nucl. Phys. B* **483**, 291–320 (1997).
- [50] B. G. Zakharov, *JETP Letters* **63**, 952–957 (1996) [*Pis'ma Zh. Eksp. Teor. Fiz.* **63**, 906–910 (1996)].
- [51] R. Baier, Yu. Dokshitzer, S. Peigné and D. Schiff, *Phys. Lett. B* **345**, 277–286 (1995).
- [52] R. Baier *QCD*, *Proc. IV Workshop-1998 (Paris)* Eds, H. M. Fried, B. Müller (World Scientific, Singapore, 1999) pp 272–279.
- [53] M. J. Tannenbaum *ibid.*, [pp 280–285](#), pp 312–319.

- [54] For example, see *Proc. Int'l Wks. Quark Gluon Plasma Signatures (Strasbourg)* Eds. V. Bernard, *et al.*, (Editions Frontieres, Gif-sur-Yvette, France, 1999).
- [55] F. W. Büsser *et al.*, *Phys. Lett. B* **46**, 471 (1973), see also *Proc. 16th Int. Conf. High Energy Physics*, Eds. J. D. Jackson and A. Roberts, (NAL, Batavia, IL, 1972) Vol. 3, p. 317.
- [56] M. Banner *et al.*, *Phys. Lett. B* **44**, 537 (1973).
- [57] B. Alper *et al.*, *Phys. Lett. B* **44**, 521 (1973).
- [58] M. J. Tannenbaum, *Particles and Fields-1979*, AIP Conference Proceedings Number 59, Eds. B. Margolis, D. G. Stairs (American Institute of Physics, New York, 1980) pp. 263–309.
- [59] S. S. Adler *et al.* (PHENIX Collaboration), *Phys. Rev. D* **74**, 072002 (2006).
- [60] M. J. Tannenbaum, *Proc. Correlations Fluctuations in Relativistic Nuclear Collisions*, Florence, Italy, July 7–9, 2006, [PoS \(CFRNC2006\) 001](#).
- [61] M. J. Tannenbaum, *How to Discover the QGP by Single particle Semi-inclusive Measurements, or, Using Leading Particles to Measure the Properties of Jets and Di-Jets*, [RHIC'97 Summer Study](#).
- [62] M. Gyulassy and M. Plümer, *Phys. Lett. B* **243**, 432 (1990).
- [63] X.-N. Wang and M. Gyulassy, *Phys. Rev. Lett.* **68**, 1480 (1992).
- [64] A. Adare, *et al.* (PHENIX Collaboration), *Phys. Rev. D* **76**, 051106(R) (2007).
- [65] A. Adare, *et al.* (PHENIX Collaboration), *Phys. Rev. D* **79**, 012003 (2009).
- [66] G. Cocconi, L. J. Koester, and D. H. Perkins, [Technical Report No.~UCRL-10022 \(1961\)](#), Lawrence Radiation Laboratory, (unpublished), p. 167.
- [67] For example, see M. J. Tannenbaum, *Int. J. Mod. Phys. A* **4**, 3377–3476 (1989).
- [68] K. Adcox *et al.*, PHENIX Collaboration *Nucl. Phys. A* **757**, 184–283 (2005).
- [69] J. D. Bjorken, *Phys. Rev. D* **27**, 140–151 (1983).
- [70] S. S. Adler, *et al.* (PHENIX), *Phys. Rev. C* **71**, 034908 (2005).
- [71] T. Abbott, *et al.* (E802), *Phys. Rev. C* **63**, 064602 (2001); *Phys. Rev. C* **68**, 034908 (2003).
- [72] M. J. Tannenbaum, *Prog. Part. Nucl. Phys.* **53**, 239–252 (2004).
- [73] K. Adcox, *et al.* (PHENIX Collab.), *Phys. Rev. Lett.* **86**, 3500 (2001).
- [74] D. Karzeev, M. Nardi, *Phys. Lett. B* **507**, 121 (2001).
- [75] A. L. S. Angelis, *et al.* (COR Collaboration), *Phys. Lett. B* **126**, 132–136 (1983).
- [76] P. Bagnia, *et al.* (UA2 Collaboration), *Phys. Lett. B* **138**, 430–440 (1984); J. A. Appel, *et al.* (UA2 Collaboration), *Phys. Lett. B* **165**, 441 (1985).
- [77] N. Armesto, N. Borghini, S. Jeon, U. A. Wiedemann, *et al.*, *J. Phys. G* **35**, 054001 (2008).
- [78] C. Alt, *et al.* (NA49 Collab.), *Phys. Rev. C* **68**, 034903 (2003).
- [79] H. Song and U. Heinz, *Phys. Rev. C* **78**, 024902 (2008).
- [80] M. Breidenbach *et al.*, *Phys. Rev. Lett.* **23**, 935 (1969). See also W. K. H. Panofsky *Proc. 14th Int. Conf. High Energy Physics-1982 (Vienna)* Eds. J. Prentki and J. Steinberger (CERN Scientific Information Service, Geneva, SZ, 1968), pp. 23–42.
- [81] J. D. Bjorken and E. A. Paschos, *Phys. Rev.* **185**, 1975–1982 (1969).

- [82] S. M. Berman, J. D. Bjorken and J. B. Kogut, *Phys. Rev. D* **4**, 3388 (1971).
- [83] R. Blankenbecler, S. J. Brodsky, J. F. Gunion, *Phys. Lett. B* **42**, 461 (1972).
- [84] R. F. Cahalan, K. A. Geer, J. Kogut and Leonard Susskind, *Phys. Rev. D* **11**, 1199 (1975).
N.B. Interestingly, this paper came to the erroneous conclusion that “single vector-gluon exchange contributes insignificantly to wide-angle hadron collisions.”
- [85] For example, see reference [60] for more details.
- [86] For example, see *Proc. XIV Rencontre de Moriond—“Quarks, Gluons and Jets” (Les Arcs)* (Editions Frontières, Dreux, France, 1979) H. Boggild, p. 321, [M. J. Tannenbaum, p. 351](#), and references therein.
- [87] A. L. S. Angelis, *et al.* (CCOR Collaboration), *Physica Scripta* **19**, 116–123 (1979).
- [88] P. Darriulat, *et al.*, *Nucl. Phys. B* **107**, 429–456 (1976).
- [89] M. Della Negra *et al.* (CCHK Collaboration), *Nucl. Phys. B* **127**, 1 (1977).
- [90] R. P. Feynman, R. D. Field and G. C. Fox *Nucl. Phys. B* **128**, 1 (1977).
- [91] P. Darriulat *Ann. Rev. Nucl. Part. Sci.* **30**, 159 (1980).
- [92] M. Jacob, *Proc. EPS Int’l Conf. HEP*, Geneva, Switzerland, 27 June–4 July, 1979 (CERN, Geneva, 1979) [Volume 2, pp. 473–522](#). See p. 512 for this figure.
- [93] T. Aaltonen *et al.* (CDF Collaboration), *Phys. Rev. D* **79**, 112005 (2009).
- [94] See p. 511 in reference [92].
- [95] For a contemporary view of the excitement of this period, and some more details, see reference [58].
- [96] J. F. Owens, E. Reya and M. Glück *Phys. Rev. D* **18**, 1501 (1978); J. F. Owens and J. D. Kimel *Phys. Rev. D* **18**, 3313 (1978).
- [97] R. P. Feynman, R. D. Field and G. C. Fox *Phys. Rev. D* **18**, 3320 (1978).
- [98] R. Cutler and D. Sivers *Phys. Rev. D* **17**, 196 (1978); *Phys. Rev. D* **16**, 679 (1977).
- [99] B. L. Combridge, J. Kripfganz and J. Ranft *Phys. Lett. B* **70**, 234 (1977).
- [100] T. Åkesson *et al.* (AFS Collaboration), *Phys. Lett. B* **128**, 354 (1983).
- [101] For example, see the review, M. J. Tannenbaum, *Int. J. Mod. Phys. A* **4**, 3377 (1989).
- [102] K. Pretzl, C. Favuzzi, *et al.*, *Proc. 20th Int. Conf. High Energy Physics (Madison, WI, 1980)*, Eds. L. Durand and L. G. Pondrom (AIP, New York, 1981), [pp. 92–97](#). C. De Marzo *et al.*, *Phys. Lett. B* **112**, 173 (1982).
- [103] *Proc. 21st Int. Conf. High Energy Physics-1982 (Paris)*, Eds. P. Petiau and M. Porneuf (Journal de Physique Colloques, Paris, 1982) *J. Phys. Colloques* **43**, C3 (1982) see J. P. Repellin [pp. C3-571–C3-578](#); also see M. J. Tannenbaum [pp. C3-134–C3-139](#), G. Wolf [pp. C3-525–C3-568](#).
- [104] A. L. S. Angelis *et al.* (CCOR Collaboration), *Nucl. Phys. B* **209**, 284–300 (1982).
- [105] J. F. Owens, *Rev. Mod. Phys.* **59**, 465–503 (1987).
- [106] L. DiLella *Ann. Rev. Nucl. Part. Sci.* **35**, 107 (1985).
- [107] M. J. Tannenbaum, *Polarized Collider Workshop*, AIP Conference Proceedings Number 223, Eds. J. Collins, S. F. Heppelman, R. W. Robinett (American Institute of Physics, New York, 1991) [pp. 201–209](#).

- [108] A. Adare *et al.* (PHENIX Collaboration), *Phys. Lett. B* **670**, 313–320 (2009).
- [109] A. Adare *et al.* (PHENIX Collaboration), *Phys. Rev. Lett.* **104**, 132301 (2010).
- [110] S. S. Adler *et al.* (PHENIX Collaboration), *Phys. Rev. Lett.* **98**, 012002 (2007).
- [111] B. I. Abelev *et al.* (STAR Collaboration), *Phys. Rev. Lett.* **97**, 252001 (2006).
- [112] R. Baier, D. Schiff and B. G. Zakharov, *Ann. Rev. Nucl. Part. Sci.* **50**, 37–69 (2000).
- [113] S. S. Adler *et al.* (PHENIX Collaboration), *Phys. Rev. Lett.* **91**, 172301 (2003).
- [114] A. Adare, *et al.* (PHENIX Collaboration), *Phys. Rev. Lett.* **104**, 132301 (2010).
- [115] G. Alexander *et al.* (OPAL Collaboration), *Z. Phys. C* **69**, 543 (1996).
- [116] P. Abreu *et al.* (DELPHI Collaboration), *Eur. Phys. J. C* **13**, 573 (2000).
- [117] M. J. Tannenbaum, *High- p_T physics at LHC*, Jyväskylä, Finland, March 23–27, 2007, [PoS \(LHC07\) 004](#).
- [118] A. Adare *et al.* (PHENIX Collaboration), *Phys. Rev. C* **78**, 014901 (2008); *Phys. Rev. C* **77**, 011901(R) (2008).
- [119] A. Adare, *et al.* (PHENIX Collaboration), *Phys. Rev. Lett.* **98**, 232302 (2007).
- [120] For example, see Ref. [118] for a discussion and list of references.
- [121] For example, see Ref. [122] and references therein.
- [122] J. Adams *et al.* (STAR Collaboration), *Phys. Rev. Lett.* **97**, 162301 (2006).
- [123] M. J. Horner *et al.* (STAR Collaboration), *J. Phys. G* **34**, S995–S998 (2007).
- [124] H. Zhang, J. F. Owens, E. Wang and X.-N. Wang, *Phys. Rev. Lett.* **98**, 212301 (2007).
- [125] Also, see, C. Marquet and T. Renk, *Phys. Lett. B* **685**, 270–276 (2010).
- [126] A. Adare *et al.* (PHENIX Collaboration), *Phys. Rev. C* **77**, 064907 (2008).
- [127] For example, see M. Gyulassy and P. Lévai *Nucl. Phys. A* **834**, 271c–222c (2010) and references therein.
- [128] M. J. Tannenbaum, *J. Phys: Conf. Series* **230**, 012037 (2010).
- [129] P. Sorensen, *J. Phys. G* **37**, 094011 (2010); *Proc. 24th Winter Wks. Nucl. Dynamics*, South Padre Island, TX, April 5-12, 2008, [[arXiv:0808.0503v1](#)].
- [130] B. Alver and G. Roland, *Phys. Rev. C* **81**, 054905 (2010).
- [131] A. Ayala, J. Jalilian-Marian, J. Magnin, A. Ortiz, G. Paic and M. E. Tejeda-Yeomans, *Phys. Rev. Lett.* **104**, 042301 (2010).
- [132] H. Fritzsche and P. Minkowski, *Phys. Lett. B* **69**, 316 (1977).
- [133] P. Aurenche, J. Ph. Guillet, E. Pilon, M. Werlen and M. Fontannaz, *Phys. Rev. D* **73**, 094007 (2006).
- [134] X.-N. Wang, Z. Huang and I. Sarcevic, *Phys. Rev. Lett.* **77**, 231–234 (1996).
- [135] T. Renk, *Phys. Rev. C* **80**, 014901 (2009).
- [136] T. Ferbel and W. R. Molzon, *Rev. Mod. Phys.* **56**, 181–221 (1984).
- [137] S. S. Adler *et al.* (PHENIX Collaboration), *Phys. Rev. Lett.* **98**, 012002 (2007).

- [138] S. S. Adler *et al.* (PHENIX Collaboration), *Phys. Rev. Lett.* **94**, 232301 (2005).
- [139] A. L. S. Angelis *et al.* (CMOR Collaboration), *Nucl. Phys. B* **327**, 541-568 (1989). See also T. Åkesson *et al.* (AFS Collaboration), *Phys. Lett. B* **118**, 178 (1982).
- [140] A. Adare *et al.* (PHENIX Collaboration), [arXiv:1006.1347v1 \[nucl-ex\]](#), *subm. Phys. Rev. D*.
- [141] N. Borghini and U. A. Wiedemann, *Nucl. Phys. A* **774**, 549–522 (2006); see also [arXiv:hep-ph/0506218v1](#).
- [142] Ya. I. Azimov, Yu. L. Dokshitzer, V. A. Khoze and S. I. Troyan, *Z. Phys. C* **31**, 213–218 (1986).
- [143] W. Braunschweig, *et al.* (TASSO Collab.), *Z. Phys. C* **47**, 187–198 (1990).
- [144] A. Adare *et al.* (PHENIX Collaboration), *Phys. Rev. Lett.* **104**, 252301 (2010).
- [145] A. Adare *et al.* (PHENIX Collaboration), *Phys. Rev. Lett.* **101**, 232301 (2008).
- [146] M. Connors *et al.* (PHENIX Collaboration), *Nucl. Phys. A* **830**, 447c–450c (2009).
- [147] B. I. Abelev *et al.* (STAR Collaboration), [arXiv:0912.1871v1 \[nucl-ex\]](#), *subm. Phys. Rev. Lett.* .